大久保卓哉, 水澤英洋, 金子清俊	変異型Creutzfeldt-Jakob病	日本臨床	62巻 (増刊号1), 痴呆症学. 2	252-256	2004
Paul Brown, Rainer Seitz, 水澤英洋, Henry Baron, 金子清俊	プリオンに関する日本と欧米の現状と今後-特に血漿分画製剤に関連して-.	JAMA	2	120-121	2004
金子清俊	BSE-最新の知見.	日本医事新報	4165	46-51	2004
八谷如美, 金子清俊	プリオン病の現況と将来	Current Concepts in Infectious Disease.	23	18-19	2004
金子清俊	BSE, SARS, 鳥インフルエンザ等の感染症とつきあう方法	環境会議	21	214-217	2004
八谷如美, 金子清俊	プリオン病治療の新たな可能性	バイオインダストリー	21	60-66	2004
金子清俊	BSE (牛海綿状脳症)とその食へのリスクについて	日本食肉加工情報	647	19-29	2004
八谷如美, 金子清俊	BSEとプリオンの増殖・感染機構	蛋白質・核酸・酵素	49	1005-1007	2004
八谷如美, 金子清俊	プリオン病とミトコンドリアの接点	医学のあゆみ	209	1015-1017	2004
金子清俊	プリオン病	小児内科	36	1166-1169	2004
金子清俊	プロテオミクスによる神経疾患の病態解析	神経研究の進歩	48	700-706	2004
金子清俊	ウシ海綿状脳症 (BSE)	現代化学	404	32-36	2004
金子清俊	プルシナー論文を読むコッホの四原則を証明	現代化学	404	39	2004

金子清俊	BSE検査	日本医事新報	4200	88-89	2004
金子清俊	クロイツフェルト・ヤコブ病.	臨床と微生物	32	69-72	2005
八谷如美, 金子清俊	新しいシャペロンの発見 - 神経難病の治療へ-.	科学	75	283-285	2005
金子清俊	プリオンタンパク，プリオン遺伝子	医学大辞典			印刷中
金子清俊	プリオン病	Medical View			印刷中
金子清俊	牛海綿状脳症/プリオン病.	日本内科学会誌			印刷中
金子清俊	Prion病の治療法開発	先端医療	第10章		印刷中
逆瀬川裕二，八谷如美，金子清俊	プリオン病	国立医療学誌「医療」			印刷中
八谷如美, 金子清俊	プリオン研究の進展.	VIRUS REPORT			印刷中
桑田　一夫	プリオン中間体と治療薬開発ー分子感染機構と創薬制御	蛋白質　核酸　酵素	49(7)	1110-1112	2004
桑田　一夫	素数とプリオンー21世紀における生命科学の新表現理論への挑戦	数理化学	499	45-53	2005

Available online at www.sciencedirect.com
SCIENCE DIRECT®
Biochemical and Biophysical Research Communications 313 (2004) 818–823
BBRC
www.elsevier.com/locate/ybbrc

Microtubules-associated intracellular localization of the NH_2-terminal cellular prion protein fragment

Naomi S. Hachiya, Kota Watanabe, Yuji Sakasegawa, and Kiyotoshi Kaneko*

Department of Cortical Function Disorders, National Institute of Neuroscience (NIN), National Center of Neurology and Psychiatry (NCNP), Tokyo 187-8502, Japan
Core Research for Evolutional Science and Technology (CREST), Japan Science and Technology Corporation, Japan

Received 25 November 2003

Abstract

By utilizing double-labeled fluorescent cellular prion protein (PrP^C), we revealed that the NH_2-terminal and COOH-terminal PrP^C fragments exhibit distinct distribution patterns in mouse neuroblastoma neuro2a (N2a) cells and HpL3-4, a hippocampal cell line established from *prnp* gene-ablated mice [Nature 400 (1999) 225]. Of note, the NH_2-terminal PrP^C fragment, which predominantly localized in the intracellular compartments, congregated in the cytosol after the treatment with a microtubule depolymerizer (nocodazole). Truncated PrP^C with the amino acid residues 1–121, 1–111, and 1–91 in mouse (Mo) PrP exhibited a proper distribution profile, whereas those with amino acid residues 1–52 and 1–33 did not. These data indicate the microtubules-associated intracellular localization of the NH_2-terminal PrP^C fragment containing at least the 1–91 amino acid residues.

Keywords: Prion protein; Microtubules; Fluorescent protein; Nocodazole; Proteolytic cleavage; Subcellular localization

Prion diseases are a group of neurodegenerative disorders including kuru, Creutzfeldt–Jakob disease (CJD), Gerstmann–Sträussler–Scheinker disease (GSS), and fatal familial insomnia (FFI) in humans, scrapie in sheep, and bovine spongiform encephalopathy (BSE) in cattle, which can be presented as sporadic, inherited, and infectious disorders [2]. The posttranslational conformational change of the cellular isoform of prion protein (PrP^C) into the scrapie isoform of prion protein (PrP^{Sc}) is the fundamental process underlying the pathogenesis of the prion disease [3,4]. After PrP^C is synthesized in the endoplasmic reticulum, it transits through the Golgi apparatus to the cell surface lipid rafts which is a subcellular compartment defined biochemically by membranes rich in cholesterol and glycosphingolipids, where it is bound by a glycophosphatidylinositol (GPI)-anchor [5,6] and then PrP^C is either metabolized or converted into PrP^{Sc} [7–9].

Several groups have already generated fluorescent PrP^C molecules, in which a green fluorescent protein (GFP) was either NH_2-terminally or COOH-terminally fused [10–13]. Of note, the copper treatment induced fluorescent PrP^C to be internalized like endogenous PrP^C, indicating that such fluorescent PrP^C could be functional [10]. Regardless of the position of the GFP inserts, fluorescent PrP^C in a GPI-anchored form was reported as being correctly targeted to the plasma membrane, where it is detected in lipid rafts [10,12]. However, there has been neither direct comparison of distribution profiles between NH_2-terminally and COOH-terminally fluorescent-tagged PrP^C.

With this background, we made fluorescent PrP constructs double-labeled at both NH_2- and COOH-termini, and then investigated the subcellular localization in mouse neuroblastoma neuro2a (N2a) cells, known to be infectable with PrP^{Sc} [14], and HpL3-4, a hippocampal cell line established from *prnp* gene-ablated mice [1]. Subsequently, we are tempted to investigate the association of the NH_2-terminal PrP^C fragment with cytoskeletal proteins such as microtubules and actin.

* Corresponding author. Fax: +81-42-346-1748.
E-mail address: kaneko@ncnp.go.jp (K. Kaneko).

0006-291X/$ - see front matter © 2003 Elsevier Inc. All rights reserved.
doi:10.1016/j.bbrc.2003.11.167

Materials and methods

Construction of fluorescent PrP and the deletion mutants. To express fluorescent PrP in mouse neuroblastoma cells, the EGFP gene was amplified by PCR from pEGFP (Clontech) using primers 5′-GACC GGTATGGTGAGCAAGGGCGAGGAGCTG-3′ and 5′-GACCG GTATGGTGAGCAAGGGCGAGGAGCTG-3′, digested with *Age*I, and inserted into the *Age*I site (between amino acid residues 34 and 35 in mouse (Mo) PrP) of pSPOX-MHM2PrP (a gift from Dr. S.B. Prusiner, University of California, San Francisco) [15] and the resulted plasmid was designated pSPOX-MHM2PrP::GFP. The series of deletion mutants were amplified by PCR from the pSPOX-MHM2PrP::GFP using 5′-CGGGATCCACCATGGCGAACCTTG GCTACTGGCTG-3′ as the forward primer and the following backward primers: 5′-CCG CTCGAGTCACTTGTACAGCTCGTCCATGCCGAGA-3′ (for amino acid residues 1–33 in Mo PrP), 5′-CCGCTCGAGTCACTGA GGTGGGTAACGGTT-3′ (1–52), 5′-CCGCTCGAGTCATCCTTG GCCCCATCCACC-3′ (1–91), 5′-CCGCTCGAGTCACATATGCTT CATGTTGGT-3′ (1–111), and 5′-CCGCTCGAGTCACACTACTG CCCCAGCTGC-3′ (1–121), digested with *Bam*HI and *Xho*I, and replaced with the *Bam*HI–*Xho*I fragment of pSPOX-MHM2PrP::GFP. The resulted plasmids were verified by direct DNA sequencing.

Antibodies, organelle markers, and drugs. Anti-PrP antibodies K1, K3, and K9 were rabbit polyclonal serum raised against the NH_2-termianl PrP peptides (amino acid residues 26–40, 76–90, and 196–210 in Mo PrP, respectively). Anti-COOH-terminal polyclonal PrP^C antibody M20 and anti-tubulin antibody DM1A were purchased from Santa Cruz Biotechnology and Sigma, respectively. A Golgi marker anti-GM130 and a marker for lipid raft anti-GM1 antibody were purchased from BD Biosciences and Calbiochem, respectively. As ER markers, ER-Tracker Blue-White DPX (Molecular Probes), Calnexin (Stressgen), BiP (BD Biosciences), and PDI (Stressgen) were purchased and used. Other organelle markers including an early endosomal marker EEA1 (BD Biosciences), a lysosomal marker LysoTracker Green (Molecular Probes), and a mitochondrial marker MitoTracker Red CHXROS (Molecular Probes) were also used for the experiments. Nocodazole was purchased from Sigma.

Cell cultures, DNA transfection, and drug treatments. Mouse neuroblastoma neuro2a (N2a) cells were obtained from American Tissue Culture Collection. A hippocampal cell line established from *prnp* gene-ablated mice (HpL3-4) was kindly provided by Dr. T. Onodera. Cells were grown and maintained at 37 °C in MEM supplemented with 10% fetal bovine serum. N2a and HpL3-4 cells were transiently transfected with each construct using a DNA transfection kit (Lipofectamin, Gibco-BRL). Western blot analyses were performed as described [15]. Nocodazole treatment (30 μM at 30 °C for 0, 30, and 180 min) was performed according to the previous report [16].

Immunofluorescent and fluorescence microscopy. For indirect immunofluorescence analysis, fluorescent PrP^C-transfected cells were rinsed with PBS with Ca^{2+} and Mg^{2+} (PBS(+)) and then fixed with 10% formalin in 70% PBS(+) at room temperature for 30 min. After four washes with PBS(−), the fixed cells were incubated with 10% FBS in PBS(−) at room temperature for 30 min. They were then incubated at room temperature for 1 h with antibodies at desired concentrations. After four washes with PBS(−), the cells were incubated with either Alexa488 (green) Fluor-conjugated anti-rabbit IgG (Molecular Probes) or Alexa594 (red) Fluor-conjugated anti-mouse IgG (Molecular Probes), diluted 1:200 in PBS, at room temperature for 1 h. The stained cells were washed four times with PBS(−) and mounted with SLOW FADE (Molecular Probes). Immunofluorescent or autofluorescent samples were imaged with Delta-Vision microscopy system (Applied Precision), out of focus light of the visualized images was removed by interactive deconvolution.

Immunoprecipitation of tubulin and PrP^C from the tubulin–PrP^C containing vesicular complex. Harvested N2a cells (13 dishes of 9 cm plate) were washed with PBS(−) twice, suspended in PEM buffer (100 mM Pipes, 2 mM EDTA, and 1 mM $MgCl_2$) containing protease inhibitors (5 μM each of leupeptin, pepstatin, aprotinin, antipain, and 1 mM PMSF), and homogenized 30 times at 4 °C. The homogenates were centrifuged at 3000*g* for 3 min followed by 100,000*g* at 4 °C for 30 min and then the supernatant was recovered. To stabilize tubulin, the supernatant was treated with taxol (20 μM) with 1 mM GTP at 37 °C for 20 min and kept on ice for 10 min. Monoclonal anti-tubulin antibody DM1A was adsorbed to protein A–cellurofine in PBS at 4 °C for 5 h and then used for the immunoprecipitation. PrP^C signals were detected by Western blotting with either K1 or K9 from the immunoprecipitated complex. Polyclonal K1 and K9 are suitable for Western blotting (data not shown).

Results

Subcellular localization of fluorescent PrP^C

The subcellular localization of fluorescent PrP^C was investigated by utilizing double-labeled PrP^C, GFP–PrP–DsRed, and vice versa in N2a cells (Fig. 1A). We detected a NH_2-terminal PrP^C fragment predominantly in intracellular compartments as a dot-like distribution pattern, a COOH-terminal PrP^C fragment mostly at the cell surface, and PrP^C in full length intracellularly (Fig. 1B). These results were in accordance with the behavior of endogenous PrP^C immunostained with anti-PrP polyclonal antibodies K3 against the NH_2-terminal residues 76–90 in Mo PrP (Fig. 1C, left panel), and M20 against the COOH-terminal residues in Mo PrP (Fig. 1C, right panel) and thus, excluding the possibility of an artificial distribution of fluorescent PrP^C by fusing the fluorescent proteins.

While a large proportion of intracellular PrP^C was co-localized with a Golgi marker (anti-GM130) (data not shown), signals on plasma membranes were co-localized with a marker for lipid rafts (anti-GM1) (data not shown). These results are consistent with the previous observations [11–13,17]. However, under our culture conditions with N2a and HpL3-4 cells, we were unable to demonstrate co-localization of the intracellular NH_2-terminal PrP^C fragment in a dot-like distribution pattern with known organelle markers such as ER (ER-Tracker Blue-White DPX, Calnexin, BiP, PDI), Golgi apparatus (GM130), early endosomes (EEA1), lysosomes (LysoTracker, Green), or mitochondria (MitoTracker Red CHXROS) (data not shown). Thus, such intracellular PrP^C may not reflect the distribution to any single specific organelle, but further examination has yet to be required.

Western blot analysis with polyclonal antibody K1 against the NH_2-terminal residues 26–40 in Mo PrP detected the NH_2-terminal PrP^C fragment of 17 kDa exclusively in a non-lipid raft fraction (data not shown). Further mapping of the NH_2-terminal PrP^C cleavage site was achieved by transiently expressing 3F4 (amino acids 108/111 in Mo PrP) [18] epitope-tagged MHM2 PrP^C in N2a cells. Again, 3F4 detected the NH_2-terminal PrP^C fragment in the non-lipid raft fraction (Fig. 1D). Taken together, these data indicate that such NH_2-terminal

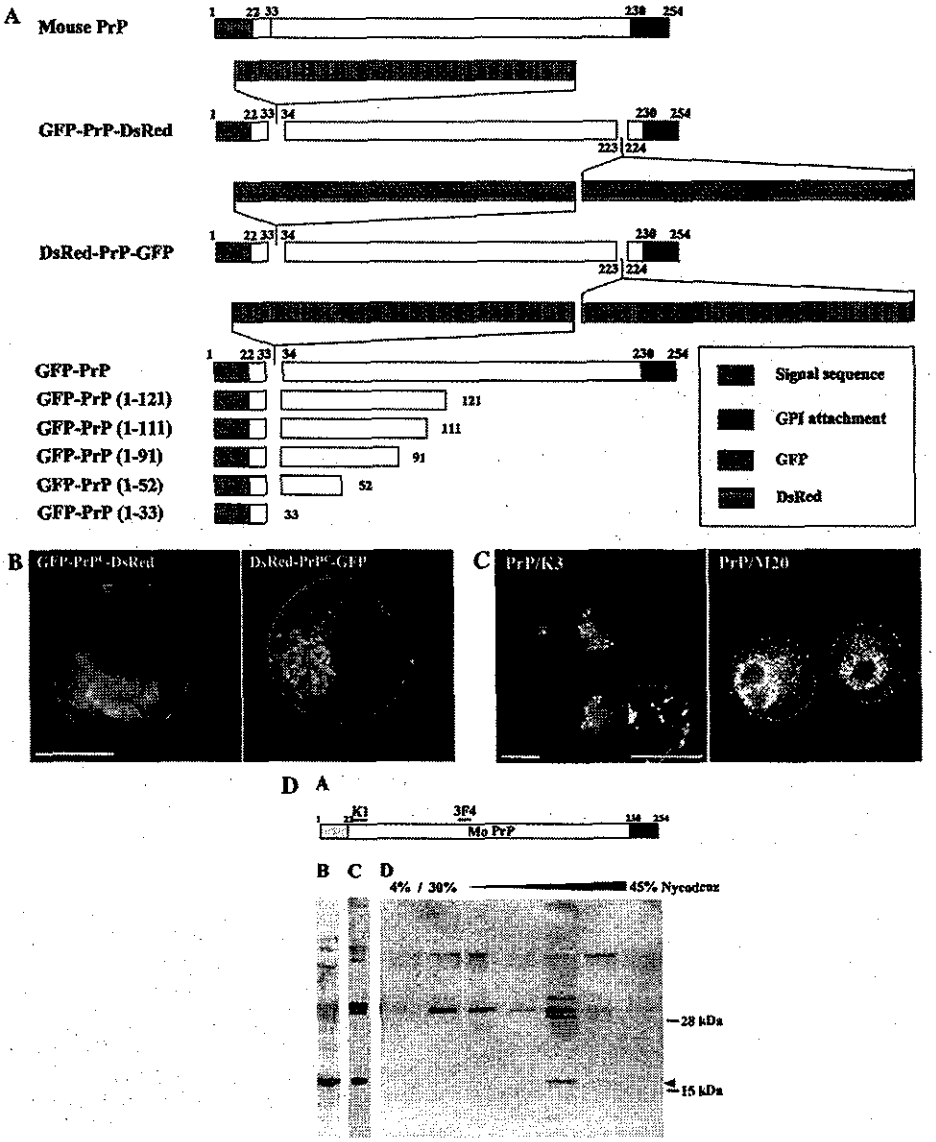

Fig. 1. Immunofluorescent analysis of fluorescent PrP^C: (A) The chimeric fluorescent PrP constructs (GFP–PrP–DsRed, DsRed–PrP–GFP, and the deletion mutant series,) used in this study. (B) Distribution patterns of GFP–PrP–DsRed (left panel): GFP–PrP^C (green) predominantly in the intracellular vesicles, PrP^C–DsRed (red) mostly at the cell surface membranes, and GFP–PrP^C–DsRed (yellow) in intracellular compartments. The DsRed–PrP–GFP (right panel) exhibits an inverted color profile indicating the same distribution patterns independent of the fluorescent conjugates. Scale bar = 8 μm. (C) Endogenous PrP^C is immunostained with anti-PrP polyclonal antibody K3 at a dilution of 1:200 (left panel) or M20 at a dilution of 1:200 (right panel). N2a cells were permeabilized with 0.1% Triton X-100. A distinct proportion of PrP^C is detected in a dot-like distribution pattern (an arrow). Scale bars = 15 μm. (D) 3F4 detects NH_2-terminal MHM2 PrP^C fragment of 17 kDa (arrow head) which was transiently transfected in N2a cells. To separate non-lipid raft fractions which contain high density, Triton X-100-insoluble intracellular membranes, we used the procedure of Naslavsky et al. [33] with slight modifications as below. Cells were lysed and resuspended in ice-cold buffer A (25 mM Hepes–KOH, pH 7.5, 5 mM EDTA, and 0.15 M NaCl) containing 1% Triton X-100, and then adjusted to 50% Nycodenz containing buffer A. Samples were centrifuged at 200,000*g* at 4 °C for 4 h by floatation in 1.5 ml of a discontinuous Nycodenz gradient (4/30/32.5/35/37.5/40/42.5/45%). After the centrifugation, samples were fractionated by 0.2 ml from the top of gradients.

PrP^C fragment contains at least residues 26–40, 76–90, and 108/111 in Mo PrP.

Microtubules-dependent intracellular localization of fluorescent PrP^C

These observations of the intracellular NH_2-terminal PrP^C fragment in a dot-like distribution pattern prompted us to further investigate its possible association with cytoskeletal proteins such as microtubules or actin. Co-immunostaining of endogenous PrP^C and microtubules by anti-PrP polyclonal antibody K3/anti-tubulin monoclonal antibody DM1A detected PrP^C along microtubules in N2a cells (Fig. 2) as well as HpL3-4 cells (data not shown). Subsequently, an immunoprecipitation assay performed with anti-tubulin antibody

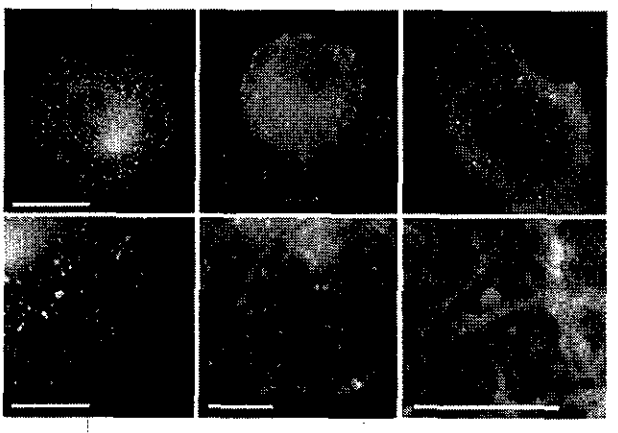

Fig. 2. Co-immunostaining of endogenous PrP^C and microtubules by anti-PrP antibody K3 (1:200, green) and anti-tubulin antibody DM1A (1:200, red) detects PrP^C along microtubules in N2a cells. Scale bar (upper panels) = 7 μm and scale bars (lower panels) = 3 μm.

(DM1A) resulted in the co-immunoprecipitation of tubulin and the NH_2-terminal PrP^C fragment of 17 kDa in N2a cells (Fig. 3A). Another polyclonal antibody K9 against the COOH-terminal residues 196–210 in Mo PrP failed to detect COOH-terminal PrP^C in the immunoprecipitated complex (Fig. 3A).

After N2a cells (Fig. 3B) were treated with 30 μM nocodazole which depolymerizes microtubules, the signals of GFP–PrP^C were congregated in a time-dependent manner. On the other hand, latrunculin A, which is widely used as an agent to sequester monomeric actin in living cells, did not affect the localization of GFP–PrP^C (data not shown). Finally, the deletion mutants (Fig. 1A) were used to map the amino acid residues responsible for the microtubules-associated localization of GFP–PrP^C. As shown in Fig. 3C, truncated constructs with the amino acid residues 1–121, 1–111, and 1–91 in Mo PrP exhibited its proper localization, whereas those with amino acid residues 1–52 and 1–33 in Mo PrP lost the dot-like distribution pattern.

Discussion

First of all, our double-labeled fluorescent PrP^C detected the NH_2-terminal and COOH-terminal PrP^C fragments with distinct subcellular distribution profiles, in which cleavage of PrP^C at around a middle region was involved [7,19,20].

Initial studies performed on the internalization of PrP^C using a chicken PrP^C have determined that endocytosis of chicken PrP is mediated by clathrin-coated pits, and the NH_2-terminal half of the chicken PrP polypeptide is essential for its endocytosis [21,22]. Recently, Nunziante et al. [23] also reported that the

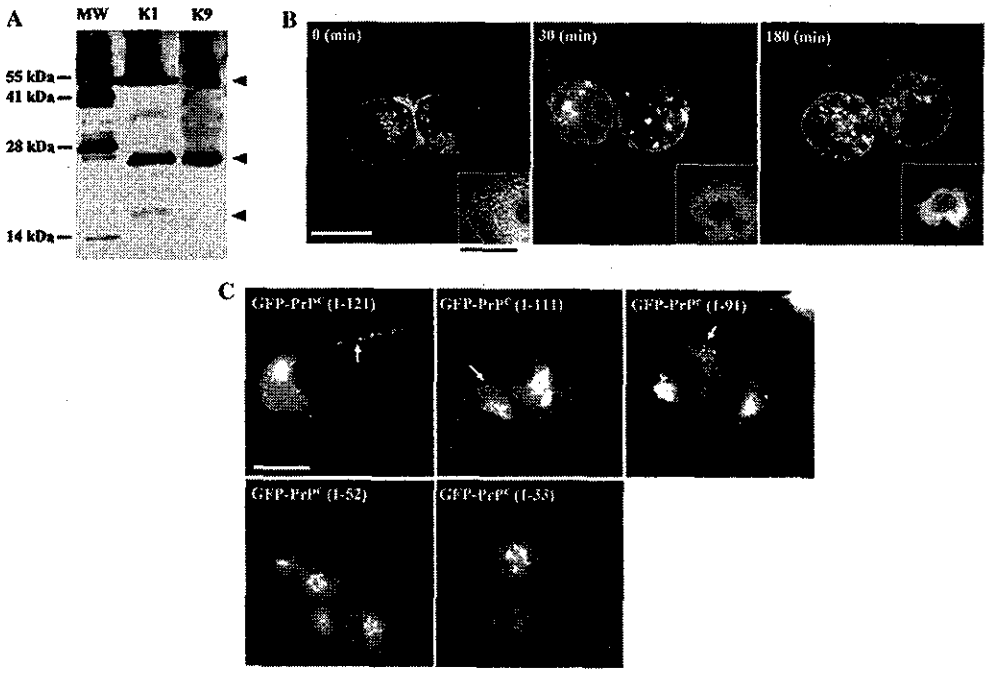

Fig. 3. The association of intracellular GFP–PrP^C with microtubules. (A) Co-immunoprecipitation of tubulin and the NH_2-terminal PrP^C fragment. Anti-tubulin antibody DM1A is used for the immunoprecipitation, and a polyclonal antibody K1 (1:500) against PrP residues 26–40 but not K9 (1:500) against residues 196–210 detects the NH_2-terminal PrP^C fragment of 17 kDa (lower arrow head) in the immunoprecipitated complex. Both K1 and K9 detect full length PrP^C (middle arrow head) and DM1A (1:2000) detects tubulin (upper arrow head). (B) After N2a cells were treated with 33 μM nocodazole and permeabilized with 0.1% Triton X-100, signals of GFP–PrP^C congregate in a time-dependent manner (0–180 min). Panels at the lower right corners represent depolymerized microtubules stained with anti-tubulin antibody DM1A (1:200). Scale bars = 15 μm. (C) The truncated GFP–PrP constructs with the amino acid residues 1–121, 1–111, and 1–91 in Mo PrP exhibit its proper localization (arrows), whereas those with 1–52 and 1–33 lose its dot-like distribution pattern. Scale bar = 15 μm.

N-proximal domain of the PrP functions as a putative targeting element and is essential for both transport to the plasma membrane and modulation of endocytosis. Along with these observations, GFP-tagged version of PrP^C was found to be properly anchored at the cell surface and its distribution pattern was similar to that of the endogenous PrP^C, with labeling at the plasma membrane and in an intracellular perinuclear compartment [10]. Further investigation concluded that PrP^C internalizes via a dynamin-dependent endocytic pathway and that the protein is targeted to the recycling endosomal compartment via Rab5-positive early endosomes and thus, traffic of GFP–PrP^C is delivered to classic endosomes after internalization [17]. Under our culture conditions, however, we could not demonstrate co-localization of the NH_2-terminal PrP^C fragment with any single specific organelle so far examined.

With this background, we have shown the microtubules-dependent intracellular localization of the NH_2-terminal PrP^C fragment in the cells. However, the question how intracellular PrP^C actually interacts with microtubules still remains to be examined. After internalized, the NH_2-terminal PrP^C fragment seems to reside inside vesicles where integral membrane proteins and linker proteins in some cases, for example, Jun kinase-interacting proteins (JIPs) [24,25], would be required for the interaction with microtubules to bridge the luminal and cytoplasmic phases across the membranes [26]. So far, we have not identified such intervening molecule/s involved in the PrP^C–microtubule interaction. Alternatively, a transmembrane form of PrP^C may be engaged in the direct interaction with the microtubules. It was suggested that a transmembrane form of PrP^C, termed C-transmembrane (^{ctm}PrP), has the COOH-terminus in the lumen with the NH_2-terminus accessible to proteases in the cytosol produced neurodegenerative changes in mice similar to those of some genetic prion diseases [27]. Such ^{ctm}PrP exposes its NH_2-terminus to the cytosol where the ^{ctm}PrP–microtubule interactions could theoretically occur, although it is less likely, as such transmembrane ^{ctm}PrP is rather pathogenic than physiologic. The fact that the truncated PrP^C with residues 1–91 cannot form ^{ctm}PrP [27], but still exhibits the microtubules-associated intracellular localization, also does not support the notion. Interestingly, these residues 1–91 partly overlap with an octapeptide repeat region, which is related to the copper metabolism [28–32]. Finally, it is also indispensable for identifying how many NH_2-terminal PrP^C fragments reside in each dot-like vesicle.

In summary, we demonstrated the microtubules-associated intracellular localization of NH_2-terminal PrP^C fragment at a steady state level. At the same time, a real time imaging analysis of fluorescent PrP^C in living cells has yet to be done toward further understanding of its mode of existence and dynamics along the microtubular network.

Acknowledgments

We greatly thank S.B. Prusiner and D.A. Harris for discussions and comments, T. Onodera for providing us the HpL3-4 cell line, M. Kawabata, E. Nannri, C. Ota, and Y. Yamaura for technical assistances. This work was supported by grants from the Core Research for Evolutional Science and Technology (CREST) of Japan Science and Technology Agency, Health and Labour Sciences Research Grants, Research on Advanced Medical Technology, nano-001, and the Ministry of Health, Labor, and Welfare of Japan.

References

[1] C. Kuwahara, A.M. Takeuchi, T. Nishimura, K. Haraguchi, A. Kubosaki, Y. Matsumoto, K. Saeki, T. Yokoyama, S. Itohara, T. Onodera, Prions prevent neuronal cell-line death, Nature 400 (1999) 225–226.
[2] S.B. Prusiner, Prions, Proc. Natl. Acad. Sci. USA 95 (1998) 13363–13383.
[3] S.B. Prusiner, D.C. Bolton, D.F. Groth, K.A. Bowman, S.P. Cochran, M.P. McKinley, Further purification and characterization of scrapie prions, Biochemistry 21 (1982) 6942–6950.
[4] S.B. Prusiner, P. Peters, K. Kaneko, A. Taraboulos, V. Lingappa, F.E. Cohen, S.J. DeArmond, Cell biology of prions, in: S.B. Prusiner (Ed.), Prion Biology and Diseases, Cold Spring Harbor, New York, 1999, pp. 349–391, Chap. 9.
[5] N. Stahl, D.R. Borchelt, K. Hsiao, S.B. Prusiner, Scrapie prion protein contains a phosphatidylinositol glycolipid, Cell 51 (1987) 229–240.
[6] B. Caughey, R.E. Race, D. Ernst, M.J. Buchmeier, B. Chesebro, Prion protein biosynthesis in scrapie-infected and uninfected neuroblastoma cells, J. Virol. 63 (1989) 175–181.
[7] A. Taraboulos, M. Scott, A. Semenov, D. Avrahami, L. Laszlo, S.B. Prusiner, Cholesterol depletion and modification of COOH-terminal targeting sequence of the prion protein inhibit formation of the scrapie isoform, J. Cell Biol. 129 (1995) 121–132.
[8] M. Vey, S. Pilkuhn, H. Wille, R. Nixon, S.J. DeArmond, E.J. Smart, R.G. Anderson, A. Taraboulos, S.B. Prusiner, Subcellular colocalization of the cellular and scrapie prion proteins in caveolae-like membranous domains, Proc. Natl. Acad. Sci. USA 93 (1996) 14945–14949.
[9] K. Kaneko, M. Vey, M. Scott, S. Pilkuhn, F.E. Cohen, S.B. Prusiner, COOH-terminal sequence of the cellular prion protein directs subcellular trafficking and controls conversion into the scrapie isoform, Proc. Natl. Acad. Sci. USA 94 (1997) 2333–2338.
[10] K.S. Lee, A.C. Magalhaes, S.M. Zanata, R.R. Brentani, V.R. Martins, M.A. Prado, Internalization of mammalian fluorescent cellular prion protein and N-terminal deletion mutants in living cells, J. Neurochem. 79 (2001) 79–87.
[11] L. Ivanova, S. Barmada, T. Kummer, D.A. Harris, Mutant prion proteins are partially retained in the endoplasmic reticulum, J. Biol. Chem. 276 (2001) 42409–42421.
[12] A. Negro, C. Ballarin, A. Bertoli, M.L. Massimino, M.C. Sorgato, The metabolism and imaging in live cells of the bovine prion protein in its native form or carrying single amino acid substitutions, Mol. Cell Neurosci. 17 (2001) 521–538.
[13] H. Lorenz, O. Windl, H.A. Kretzschmar, Cellular phenotyping of secretory and nuclear prion proteins associated with inherited prion diseases, J. Biol. Chem. 277 (2002) 8508–8516.
[14] D.A. Butler, M.A. Scott, J.M. Bockman, D.R. Borchelt, A. Taraboulos, K.K. Hsiao, D.T. Kingsbury, S.B. Prusiner, Scrapie-

infected murine neuroblastoma cells produce protease-resistant prion proteins, J. Virol. 62 (1988) 1558–1564.
[15] M.R. Scott, R. Kohler, D. Foster, S.B. Prusiner, Chimeric prion protein expression in cultured cells and transgenic mice, Protein Sci. 1 (1992) 986–997.
[16] T.A. Schroer, M.P. Sheetz, Role of kinesin and kinesin-associated proteins in organelle transport, in: F.D. Warner, J.R. McIntosh (Eds.), Cell Movement, Alan R. Liss, New York, 1989, pp. 295–306.
[17] A.C. Magalhaes, J.A. Silva, K.S. Lee, V.R. Martins, V.F. Prado, S.S.G. Ferguson, M.V. Gomez, R.R. Brentani, M.A.M. Prado, Endocytic intermediates involved with the intracellular trafficking of a fluorescent cellular prion protein, J. Biol. Chem. 277 (2002) 33311–33318.
[18] R.J. Kascsak, R. Rubenstein, P.A. Merz, M. Tonna-DeMasi, R. Fersko, R.I. Carp, H.M. Wisniewski, H. Diringer, Mouse polyclonal and monoclonal antibody to scrapie-associated fibril proteins, J. Virol. 61 (1987) 3688–3693.
[19] M. Rogers, D. Serban, T. Gyuris, M. Scott, T. Torchia, S.B. Prusiner, Epitope mapping of the Syrian hamster prion protein utilizing chimeric and mutant genes in a vaccinia virus expression system, J. Immunol. 147 (1991) 3568–3574.
[20] K.-M. Pan, N. Stahl, S.B. Prusiner, Purification and properties of the cellular prion protein from Syrian hamster brain, Protein Sci. 1 (1992) 1343–1352.
[21] S.-L. Shyng, J.E. Heuser, D.A. Harris, A glycolipid-anchored prion protein is endocytosed via clathrin-coated pits, J. Cell Biol. 125 (1994) 1239–1250.
[22] S.-L. Shyng, K.L. Moulder, A. Lesko, D.A. Harris, The N-terminal domain of a glycolipid-anchored prion protein is essential for its endocytosis via clathrin-coated pits, J. Biol. Chem. 270 (1995) 14793–14800.
[23] M. Nunziante, S. Gilch, H.M. Schatzl, Essential role of the prion protein N terminus in subcellular trafficking and half-life of cellular prion protein, J. Biol. Chem. 278 (2003) 3726–3734.
[24] A.B. Bowman, A. Kamal, B.W. Ritchings, A.V. Philp, M. McGrail, J.G. Gindhart, L.S. Goldstein, Kinesin-dependent axonal transport is mediated by the sunday driver (SYD) protein, Cell 103 (2000) 583–594.
[25] K.J. Verhey, D. Meyer, R. Deehan, J. Blenis, B.J. Schnapp, T.A. Rapoport, B. Margolis, Cargo of kinesin identified as JIP scaffolding proteins and associated signaling molecules, J. Cell Biol. 152 (2001) 959–970.
[26] M. Schliwa, G. Woehlke, Molecular motors, Nature 422 (2003) 759–765.
[27] R.S. Hegde, J.A. Mastrianni, M.R. Scott, K.A. DeFea, P. Tremblay, M. Torchia, S.J. DeArmond, S.B. Prusiner, V.R. Lingappa, A transmembrane form of the prion protein in neurodegenerative disease, Science 279 (1998) 827–834.
[28] D.R. Brown, K. Qin, J.W. Herms, A. Madlung, J. Manson, R. Strome, P.E. Fraser, T. Kruck, A. von Bohlen, W. Schulz-Schaeffer, A. Giese, D. Westaway, H. Kretzschmar, The cellular prion protein binds copper in vivo, Nature 390 (1997) 684–687.
[29] P.C. Pauly, D.A. Harris, Copper stimulates endocytosis of the prion protein, J. Biol. Chem. 273 (1998) 33107–33110.
[30] M.L. Kramer, H.D. Kratzin, B. Schmidt, A. Romer, O. Windl, S. Liemann, S. Hornemann, H. Kretzschmar, Prion protein binds copper within the physiological concentration range, J. Biol. Chem. 276 (2001) 16711–16719.
[31] W.S. Perera, N.M. Hooper, Ablation of the metal ion-induced endocytosis of the prion protein by disease-associated mutation of the octarepeat region, Curr. Biol. 11 (2001) 519–523.
[32] A.P. Garnett, J.H. Viles, Copper binding to the octarepeats of the prion protein. Affinity, specificity, folding, and cooperativity: insights from circular dichroism, J. Biol. Chem. 278 (2003) 6795–6802.
[33] N. Naslavsky, R. Stein, A. Yanai, G. Friedlander, A. Taraboulos, Characterization of detergent-insoluble complexes containing the cellular prion protein and its scrapie isoform, J. Biol. Chem. 272 (1997) 6324–6331.

JOURNAL OF VIROLOGY, Feb. 2004, p. 2088–2099
0022-538X/04/$08.00+0 DOI: 10.1128/JVI.78.4.2088–2099.2004

Vol. 78, No. 4

Mutant PrP^{Sc} Conformers Induced by a Synthetic Peptide and Several Prion Strains

Patrick Tremblay,[1,2]†‡ Haydn L. Ball,[1,2]†§ Kiyotoshi Kaneko,[1]‖ Darlene Groth,[1] Ramanujan S. Hegde,[3]# Fred E. Cohen,[1,4,5] Stephen J. DeArmond,[1,3] Stanley B. Prusiner,[1,2,5]* and Jiri G. Safar[1,2]

Institute for Neurodegenerative Diseases[1] and Departments of Neurology,[2] Biochemistry and Biophysics,[5] Cellular and Molecular Pharmacology,[4] and Pathology,[3] University of California, San Francisco, California 94143

Received 6 August 2003/Accepted 15 October 2003

Gerstmann-Sträussler-Scheinker (GSS) disease is a dominantly inherited, human prion disease caused by a mutation in the prion protein (PrP) gene. One mutation causing GSS is P102L, denoted P101L in mouse PrP (MoPrP). In a line of transgenic mice denoted Tg2866, the P101L mutation in MoPrP produced neurodegeneration when expressed at high levels. $MoPrP^{Sc}$(P101L) was detected both by the conformation-dependent immunoassay and after protease digestion at 4°C. Transmission of prions from the brains of Tg2866 mice to those of Tg196 mice expressing low levels of MoPrP(P101L) was accompanied by accumulation of protease-resistant $MoPrP^{Sc}$(P101L) that had previously escaped detection due to its low concentration. This conformer exhibited characteristics similar to those found in brain tissue from GSS patients. Earlier, we demonstrated that a synthetic peptide harboring the P101L mutation and folded into a β-rich conformation initiates GSS in Tg196 mice (29). Here we report that this peptide-induced disease can be serially passaged in Tg196 mice and that the PrP conformers accompanying disease progression are conformationally indistinguishable from $MoPrP^{Sc}$(P101L) found in Tg2866 mice developing spontaneous prion disease. In contrast to GSS prions, the 301V, RML, and 139A prion strains produced large amounts of protease-resistant PrP^{Sc} in the brains of Tg196 mice. Our results argue that $MoPrP^{Sc}$(P101L) may exist in at least several different conformations, each of which is biologically active. Such conformations occurred spontaneously in Tg2866 mice expressing high levels of $MoPrP^{C}$(P101L) as well as in Tg196 mice expressing low levels of $MoPrP^{C}$(P101L) that were inoculated with brain extracts from ill Tg2866 mice, with a synthetic peptide with the P101L mutation and folded into a β-rich structure, or with prions recovered from sheep with scrapie or cattle with bovine spongiform encephalopathy.

The discovery that brain fractions enriched for prion infectivity contain a protein ($rPrP^{Sc}$) that is resistant to limited proteolytic digestion advanced prion research (8, 37). N-terminal truncation of $rPrP^{Sc}$ produced a protease-resistant fragment, denoted PrP 27-30, that is readily measured by Western blotting, enzyme-linked immunosorbent assay, or immunohistochemistry. The measurement of PrP^{Sc} was dramatically changed with the development of the conformation-dependent immunoassay (CDI), which permitted detection of full-length $rPrP^{Sc}$ as well as previously unrecognized protease-sensitive forms of PrP^{Sc} (39).

The CDI depends on using anti-PrP antibodies that react with an epitope exposed in native PrP^{C} but that do not bind to native PrP^{Sc}. Upon denaturation, the buried epitope in PrP^{Sc} becomes exposed and readily reacts with anti-PrP antibodies. Using the CDI, we discovered that most PrP^{Sc} is protease sensitive, which we designate $sPrP^{Sc}$. Whether $sPrP^{Sc}$ is an intermediate in the formation of $rPrP^{Sc}$ remains to be determined. In Syrian hamsters inoculated with eight different strains of prions, the ratio of $rPrP^{Sc}$ to $sPrP^{Sc}$ was different for each strain and the concentration of $sPrP^{Sc}$ was proportional to the length of the incubation time (39).

In earlier studies, transgenic (Tg) mice, denoted Tg2866, expressing high levels of PrP(P101L) were used to model Gerstmann-Sträussler-Scheinker (GSS) disease caused by the P102L point mutation. In the brains of several lines of mice expressing high levels of PrP(P101L), no $rPrP^{Sc}$(P101L) was detectable (26, 27, 47). This was particularly perplexing since these Tg mice expressing high levels of PrP(P101L) developed all facets of prion-induced neurodegeneration, including multicentric PrP amyloid plaques. Moreover, brain extracts from ill Tg2866 mice transmitted disease to Tg196 mice expressing low levels of PrP(P101L) that infrequently developed spontaneous neurodegeneration (29).

In humans with GSS, several different mutations of the PrP gene (*PRNP*) resulting in nonconservative amino acid substitutions have been identified (23). In these patients, the clinical presentation, disease course, and amounts of $rPrP^{Sc}$ in the brain are variable. Brain extracts from humans who died of GSS were inoculated into apes and monkeys, but the transmission rates were not correlated with the levels of PrP^{Sc} in the inoculum (1, 2, 9, 32). In a limited study, GSS(P102L) was transmitted to Tg mice expressing a chimeric mouse-human (MHu2 M) PrP transgene carrying the P102L mutation but not

* Corresponding author. Mailing address: Institute for Neurodegenerative Diseases, University of California, Box 0518, San Francisco, CA 94143-0518. Phone: (415) 476-4482. Fax: (415) 476-8386. E-mail: stanley@itsa.ucsf.edu.

† These authors contributed equally to this work.

‡ Present address: Neurochem Inc., St. Laurent, QC H4S 2A1, Canada.

§ Present address: University of Texas Southwestern Medical Center, Dallas, TX 75390.

‖ Present address: National Center of Neurology and Psychiatry and Core Research for Evolutional Science and Technology, Kodaira, Tokyo 187-8502, Japan.

Present address: National Cancer Institute, Bethesda, MD 20892.

TABLE 1. Characteristics of PrP(P101L) isoforms

Characteristic	Isoform[a]		
	PrP^{c}(P101L)	$sPrP^{Sc}$(P101L)	$rPrP^{Sc}$(P101L)
PrP epitopes (residues 90–125) in native state	Exposed	Buried	Buried
Precipitatable by PTA	−	+	+
Digestion with PK at 37°C ("PK")	Dipeptides, tripeptides	Dipeptides, tripeptides	PrP^{3} 27–30
Digestion with PK at 4°C ("cold PK")	Dipeptides, tripeptides	PrP 22–24	PrP^{3} 27–30
Infectious	−	?	+

[a] ?, unknown; +, positive; −, negative.

to Tg mice expressing MHu2M PrP without the mutation (47). In another study, GSS(P102L) human prions were transmitted to Tg mice expressing MoPrP(P101L) in which the transgene was incorporated through gene replacement (31). The use of gene replacement permits all of the regulatory elements that control the wild-type (wt) MoPrP gene to modulate the expression of MoPrP(P101L). In these mice, the expression level of MoPrP(P101L) in brain is likely to be similar to that in Tg196 mice.

When we synthesized a 55-mer MoPrP peptide composed of residues 89 to 143 containing the P101L mutation and folded it under conditions favoring a β-structure, it induced neurodegeneration in Tg196 mice (29). When the peptide was not folded into a β-structure, it did not produce disease in Tg196 mice. We report here that the peptide-initiated disease in Tg196 mice could be serially transmitted to other Tg196 mice using brain extracts from the peptide-inoculated Tg196 mice. Using procedures derived from the CDI, brain extracts from inoculated Tg196 mice were found to contain $sPrP^{Sc}$(P101L), from which a 22- to 24-kDa PrP fragment was generated by limited digestion with proteinase K (PK) at 4°C and selective precipitation with phosphotungstate (PTA) (25, 39). In the interest of clarity, we have designated digestion at 4°C as "cold PK" and simply refer to standard digestion at 37°C as "PK." To aid in distinguishing $rPrP^{Sc}$(P101L) from $sPrP^{Sc}$(P101L), their properties based on the work reported here and in other previously published papers are listed in Table 1 (39, 40).

In addition to inoculating Tg196 mice with brain extracts containing $sPrP^{Sc}$(P101L) or with the MoPrP(89-143,P101L) peptide, we inoculated Tg196 with several strains of prions carrying wt $MoPrP^{Sc}$-A or $MoPrP^{Sc}$-B. The 301V strain carrying wt $MoPrP^{Sc}$-B (22) exhibited similar abbreviated incubation times in both Tg196 mice and $Prnp^{b/b}$ mice. In contrast, the RML and 139A strains carrying wt $MoPrP^{Sc}$-A showed prolonged incubation times in both Tg196 and $Prnp^{b/b}$ mice (12, 33). Regardless of the host mouse strain, the 301V, RML, and 139A prion strains produced large amounts of $rPrP^{Sc}$ in the brains of inoculated mice. Thus, the discovery of $sPrP^{Sc}$ has for the first time provided a molecular signature for GSS prions that either arise spontaneously in mice or are induced by a synthetic peptide carrying the GSS mutation.

MATERIALS AND METHODS

Source of laboratory animals. The results reported here were derived from studies using Tg(MoPrP,P101L)196/$Prnp^{0/0}$, Tg(MoPrP,P101L)2866/$Prnp^{0/0}$, Tg(MoPrP,P101L)2247/$Prnp^{0/0}$, Tg(MoPrP)4053/$Prnp^{+/+}$, Tg(MHu2M)5378/$Prnp^{0/0}$, and Tg(MHu2MPrP,P102L)69/$Prnp^{0/0}$ mice; these Tg lines are described in detail elsewhere (27, 47, 48). All PrP-deficient animals originated from Zrch $Prnp^{0/0}$ mice (11). Transgenic lines were maintained by breeding with FVB $Prnp^{0/0}$, except for Tg(MoPrP)4053/$Prnp^{+/+}$, in which the endogenous *Prnp* gene was maintained by breeding with FVB mice (Charles River Laboratories, Hollister, Calif.). Swiss CD-1 mice, which express $Prnp^{a}$, were obtained from Charles River Laboratories, and B6.I mice, which express $Prnp^{b}$, were a generous gift from G. Carlson (12). Rabbits were obtained from Western Oregon Rabbit Company (Philomath, Ore.).

Transmission studies. The RML prion strain was derived from the Chandler isolate (14) passaged in CD-1 mice. The mouse 139A prion strain, originally isolated after more than 20 passages in mice, was obtained from R. Carp (21) and serially propagated in C57BL ($Prnp^{a/a}$) mice obtained from Charles River Laboratories. The 301V prion strain, originally isolated from a cow infected with bovine spongiform encephalopathy (BSE), was obtained from H. Fraser (10) and maintained by serial passaging in B6.I mice. Brains from ill, MoPrP(89-143, P101L) peptide-inoculated Tg196 mice were obtained from previously reported experiments (29). Ten-percent (wt/vol) brain homogenates (BH) were obtained by 10 serial extrusions through 18-, 20-, and 22-gauge needles in phosphate-buffered saline (PBS) (pH 7.4). Mice were inoculated intracerebrally (i.c.) with 30 μl of 1% BH (Table 2) or with a clarified 0.5% BH (Table 3) using a 27-gauge, disposable hypodermic syringe. Alternatively, following PTA precipitation of 1 ml of BH, pellets were resuspended in 500 μl of diluent (PBS) before i.c. inoculation (Table 3). Disease diagnosis was carried out biweekly, and animals were sacrificed following evidence of progressive neurologic dysfunction (13, 41).

Treatment of brain homogenates. For biochemical analysis only, 10% BH samples were prepared in Ca^{++}- and Mg^{++}-free PBS by homogenization (three strokes of 15 s each) with a PowerGen 125 homogenizer (Fisher Scientific). Homogenates were clarified by centrifugation at 500 × *g* for 5 min on a tabletop centrifuge. Supernatants were subjected to cold PK or PK digestion alone or in conjunction with PTA precipitation. For PK digestion, 5% BH samples were incubated with 25 μg of PK (Gibco BRL no. 25530-015; Invitrogen, Carlsbad, Calif.)/ml for 1 h at 37°C. PK activity was blocked using a protease inhibitor (PI) cocktail composed of 2 μg of aprotinin and leupeptin/ml and 0.2 mM phenylmethylsulfonyl fluoride. For cold PK digestion, clarified 10% BH containing 1% NP-40 was incubated with 250 μg of PK/ml for 1 h on *ice*. Samples were treated with PI (200 μg of aprotinin and leupeptin/ml and 5 mM phenylmethylsulfonyl fluoride), transferred to five volumes of preheated PK inactivation buffer (1% sodium dodecyl sulfate [SDS], 0.1 M Tris-HCl [pH 8.9]), and incubated at 100°C for 2 min. For cold PK followed by PTA precipitation, 10% BH were treated with cold PK, and the reaction was blocked using PI. Samples were diluted with one volume of PBS–4% Sarkosyl and PTA precipitated. For ultracentrifugation, 1 ml of these samples was centrifuged at 100,000 × *g* for 1 h at 4°C. Alternatively, 1 ml was precipitated with PTA by adjusting samples to 0.3% PTA–2.5 mM $MgCl_2$, incubated at 37°C for 1 h, and centrifuged at 16,000 × *g* for 30 min. Pellets were resuspended in PBS with PI and 0.2% Sarkosyl.

For Western blot analysis, samples were diluted with one volume of 0.1 M Tris (pH 6.8)–2% mercaptoethanol–2% NP-40 and subjected to 7.2 U of PNGase F1 per 100 μg of total protein at 37°C overnight, according to the manufacturer's recommendations (Boehringer-Mannheim, Mannheim, Germany). Proteins were precipitated with 25% trichloroacetic acid and washed with acetone. Pellets were resuspended in 1% SDS–0.1 M Tris-HCl (pH 8.9) buffer for loading on an SDS polyacrylamide gel.

Immunological reagents. To take advantage of the CDI and characterize the conformational transitions associated with PrP(P101L), we sought to identify antibodies that recognize epitopes in the region of MoPrP(P101L) located between residues 89 and 143. Surprisingly, all previously described candidate antibodies for this assay (including recombinant fragment antibody D13 [35] and polyclonal antiserum 9095 [42]), which recognize wt MoPrP within these boundaries, poorly recognized MoPrP(P101L) by Western blotting (data not shown). Therefore, a polyclonal antiserum was raised in rabbits using a random-coil

TABLE 2. Effect of the P101L mutation on the generation and transmission of infectious prions

Inoculum[a,b]	Recipients[b]	PrP^C expression level[c]	Time to disease (days ± SEM)	n/n_0[d]
None	Tg(MoPrP,P101L)196	1	552 ± 34	9/32
None	Tg(MoPrP,P101L)2866	8	132 ± 2	19/19
Tg(MoPrP,P101L)2866	CD-1	1	>700	0/8
Tg(MoPrP,P101L)2866	Tg(MoPrP-A)4053	8	>700	0/7
Tg(MoPrP,P101L)2866	Tg(MoPrP,P101L)196	1	305 ± 17	10/10
Tg(MoPrP,P101L)2866	Tg(MoPrP,P101L)196	1	263 ± 12	8/8
Tg196(2866)	Tg(MoPrP,P101L)196	1	351 ± 13	8/8
Non-β-MoPrP(89-143,P101L)[e]	Tg(MoPrP,P101L)196	1	632	1/8
β-MoPrP(89-143,P101L)[e,f]	Tg(MoPrP,P101L)196	1	360 ± 30	20/20
Tg196(β-MoPrP(89-143,P101L))[g]	Tg(MoPrP,P101L)196	1	349 ± 8	8/8
Tg196(β-MoPrP(89-143,P101L))[g]	Tg(MoPrP,P101L)196	1	351 ± 9	9/9
Tg196(β-MoPrP(89-143,P101L))[g]	Tg(MoPrP,P101L)196	1	327 ± 9	8/8
CD-1(RML)	CD-1	1	131 ± 0	29/29
CD-1(RML)[f]	Tg(MoPrP,P101L)196	1	229 ± 6	6/6
Tg196(RML)[g]	Tg(MoPrP,P101L)196	1	175 ± 1	7/7
Tg196(RML)[g]	Tg(MoPrP,P101L)196	1	186 ± 3	9/9
C57(139A)	CD-1	1	144 ± 2	14/14
C57(139A)[f]	Tg(MoPrP,P101L)196	1	425 ± 4	9/9
Tg196(139A)[g]	Tg(MoPrP,P101L)196	1	179 ± 8	9/9
Tg196(139A)[g]	Tg(MoPrP,P101L)196	1	198 ± 6	9/9
CD-1(301V)	CD-1	1	230 ± 3	10/10
CD-1(301V)	B6.I	1	132 ± 1	10/10
B6.I(301V)	B6.I	1	116 ± 1	17/17
B6.I(301V)	CD-1	1	224 ± 5	8/8
B6.I(301V)[f]	Tg(MoPrP,P101L)196	1	113 ± 4	9/9
B6.I(301V)[f]	Tg(MoPrP,P101L)196	1	127 ± 2	3/3
Tg196(301V)[g]	Tg(MoPrP,P101L)196	1	130 ± 3	5/5
Tg196(301V)[g]	Tg(MoPrP,P101L)196	1	129 ± 1	4/4

[a] Original prion inocula (RML, 139A, 301V) were obtained from *Prnp*^{a} (C57, CD-1) and/or *Prnp*^{b} mice (B6.I) or from spontaneously ill Tg(MoPrP,P101L)2866 mice. Homogenates used for transmissions originated from spontaneously ill or prion-inoculated mice at time of disease onset. The prion strain is shown in parentheses and the text preceding the parenthesis indicate the host in which it was last propagated.

[b] All Tg(MoPrP,P101L) mice were *Prnp*$^{0/0}$.

[c] Levels of PrP^C expression are compared with that of adult, wt FVB mice.

[d] Number of ill mice (n) over the total number of mice under observation (n_0).

[e] Data from reference 29.

[f] These inoculations correspond to the primary transmissions.

[g] Inocula used for these secondary transmissions were prepared from brains obtained in the primary transmissions from spontaneously ill or prion-inoculated mice at time of disease onset.

MoPrP(89-143,P101L) peptide. Four rabbits preselected for the low reactivity of their sera against homogenates from wt mouse brains were immunized subcutaneously with 1 ml of the MoPrP(89-143,P101L) peptide (250 μg/ml in PBS-RIBI adjuvant). This procedure was performed three times at 3-week intervals. Rabbits were bled 14 days after the final immunization procedure, and their sera were tested by Western blotting for reactivity against MoPrP(P101L). The serum from rabbit 5449 displayed strong reactivity against MoPrP(P101L), MHu2M(P102L), and HuPrP(P102L) but not against wt controls (Fig. 1). The epitope mapping with overlapping synthetic peptides demonstrated two dominant epitopes: one between residues 94 and 108 and a second between residues 129 and 143 (data not shown). Western blot analyses were performed as previously described (4), using anti-PrP 3F4 monoclonal antibody at a 1:2,500 dilution (30), RO73 polyclonal antiserum at a 1:5,000 dilution (43), or 5449 polyclonal antiserum at a 1:1,000 dilution. Blots were developed using the enhanced chemiluminescence system (Amersham Life Science, Arlington Heights, Ill.).

Detection of PrP^{Sc} by the CDI. Samples were processed for the CDI using time-resolved fluorescence spectroscopy, as previously described (39). Samples were split into two aliquots, one of which was kept untreated (native) while the second (denatured) was treated with one volume of 8 M guanidinium hydrochloride and heated at 80°C for 5 min. Both aliquots were further diluted 20-fold with a water-PI mixture. Samples were loaded in triplicates on 96-well polystyrene microplates (OptiPlate HTRF-96; Perkin-Elmer, Boston, Mass.) that were either precoated with the R1 recombinant fragment antibody (35) or preactivated with gluteraldehyde (0.2% in PBS [pH 7.4]; 2 h). The plates were incubated for 2 h at room temperature and blocked overnight with Tris-buffered saline (20 mM Tris-HCl [pH 7.5], 1% bovine serum albumen, 6% sorbitol) at 4°C. Primary antibodies were then added to the plates. The anti-PrP RO73 polyclonal antiserum was used at a 1:1,000 dilution with R1-coated plates, and the 5449 polyclonal antiserum was used at a 1:1,000 dilution on gluteraldehyde-activated plates, for 2 h at 37°C. Plates were washed three times with TBS–0.05% Tween 20 and incubated for 1 h with a Europium (Eu)-labeled, anti-rabbit antibody (Delfia, no. AD0105; 1:5,000). Plates were washed seven times with a Eu enhancement solution (Wallac, Turku, Finland) and read using a Discovery fluorescence detector (Perkin-Elmer). The difference in binding between the native (N) and denatured (D) states is expressed as the D:N ratio. A mathematical model was developed to calculate the β-sheet content in PrP using these values (39). The concentration of PrP in the samples was calculated from calibration curves generated with the β-rich recombinant MoPrP(89-231) for RO73 or with synthetic MoPrP(89-143,P101L) for 5449. The signal obtained from normal Tg(MoPrP,P101L)196/*Prnp*$^{0/0}$ was used as an internal reference between plates.

Histopathological procedures. Brains were removed from euthanatized animals shortly after death and were frozen on dry ice or immersion fixed in 10% buffered formalin for inclusion in paraffin. Histoblots were performed on 10-μm, frozen coronal sections, transferred to a nitrocellulose membrane, and processed for immunohistochemistry using anti-PrP RO73 polyclonal antiserum, as previously described (45). Eight-micrometer paraffin sections were stained with hematoxylin and eosin for evaluation of neurodegenerative changes. Evaluation of reactive astrocytic gliosis was performed by immunostaining of glial fibrillary

TABLE 3. Propagation of GSS(P101L) prions in transgenic mice

Inoculum[a]	Treatment	Time to disease (days ± SEM)	n/n_0[b]	Time elapsed (days)
Tg196[c]	None	478 ± 37	6/7	>500
	PTA	432	1/8	>550
	PK/PTA	468 ± 22	2/9	>500
	PTA/PK	483	1/9	>500
Tg2866[d]	None	305 ± 17	10/10	
	PTA	278 ± 16	10/10	
	PK/PTA	262 ± 12	8/8	
	PTA/PK	226 ± 8	10/10	
Tg196(2866)[e]	None	351 ± 13	8/8	
	PTA	294 ± 4	9/9	
	PK/PTA	286 ± 3	10/10	
	PTA/PK	279 ± 7	9/9	
Tg196(196(301V))[f]	None	144 ± 4	6/7	>550
	PTA	148 ± 6	7/7	
	PK/PTA	126 ± 3	5/5	
	PTA/PK	131 ± 3	8/8	

[a] All transmissions were carried out using Tg(MoPrP,P101L)196/$Prnp^{0/0}$ mice as recipients. For each inoculum series, a pool of at least three brain homogenates was split among the following treatments: none, untreated; PTA, sodium phosphotungstate precipitation; PK/PTA, PK digestion followed by PTA precipitation; PTA/PK, PTA precipitation followed by PK digestion.

[b] Number of ill animals (n) over number of animals under observation (n_0).

[c] Samples from clinically normal Tg(MoPrP,P101L)196/$Prnp^{0/0}$ mice age-matched with ill Tg196(2866) mice at ~300 days of age.

[d] Tg2866 corresponds to spontaneously ill Tg(MoPrP,P101L)2866/$Prnp^{0/0}$ mice at ~130 days of age.

[e] Tg196(2866) corresponds to ill Tg(MoPrP,P101L)196/$Prnp^{0/0}$ mice (~300 days of age) following inoculation with brain homogenates from spontaneously ill Tg2866 mice.

[f] Tg196(196(301V)) inoculum was obtained from the secondary transmission of 301V prions into Tg(MoPrP,P101L)196/$Prnp^{0/0}$ mice (see Table 1).

acidic protein using a rabbit antiserum (Dako, Carpinteria, Calif.), as previously described (34). Hydrolytic autoclaving immunodetections were carried out on paraffin-embedded sections (34).

RESULTS

Serial passage of peptide-induced GSS in Tg196 mice. In earlier studies, we reported that the i.c. inoculation of a 55-mer peptide, designated MoPrP(89-143,P101L), carrying the P101L mutation and folded into β-rich conformation, induces central nervous system (CNS) degeneration in Tg196 mice (Table 2) (29). All of the Tg196 mice succumbed to disease at ~360 days after inoculation with this peptide. Approximately 30% of uninoculated Tg196 mice developed disease at ~550 days of age.

Brain homogenates from three Tg196 mice that developed disease after peptide inoculation were inoculated into three separate groups of Tg196 mice. All of the mice developed disease, with similar mean incubation periods of 327 days, 349 days, and 351 days (Table 2). These results argue convincingly that the β-rich MoPrP(89-143,P101L) peptide induces the accumulation of infectious prions that can be serially propagated in Tg196 mice. We conclude from these findings that the β-rich 55-mer peptide either initiated the formation of de novo GSS prions in the host or is itself a synthetic prion.

Overexpression of MoPrP(P101L) induces spontaneous neurodegeneration. When high levels of MoPrP(P101L) were expressed in the brains of Tg2866 mice, mice developed spontaneous neurodegeneration at ~130 days of age. Extracts prepared from the brains of two ill Tg2866 mice inoculated into two groups of Tg196 mice caused disease in 263 days and 305 days.

Neuropathology of Tg196 mice. Often, prion strains can be distinguished by the histopathological distribution of lesions, the pattern of PrP^{Sc} accumulation, and the presence and type of amyloid plaques produced in infected brains (20) (Fig. 2). Tg196 mice inoculated with brain extracts prepared from spontaneously ill Tg2866 mice showed neuropathologic changes similar to those of Tg196 mice inoculated with the MoPrP (89-143,P101L) peptide (Fig. 2B and C). Tg196 mice that developed disease after inoculation with the MoPrP(89-143,

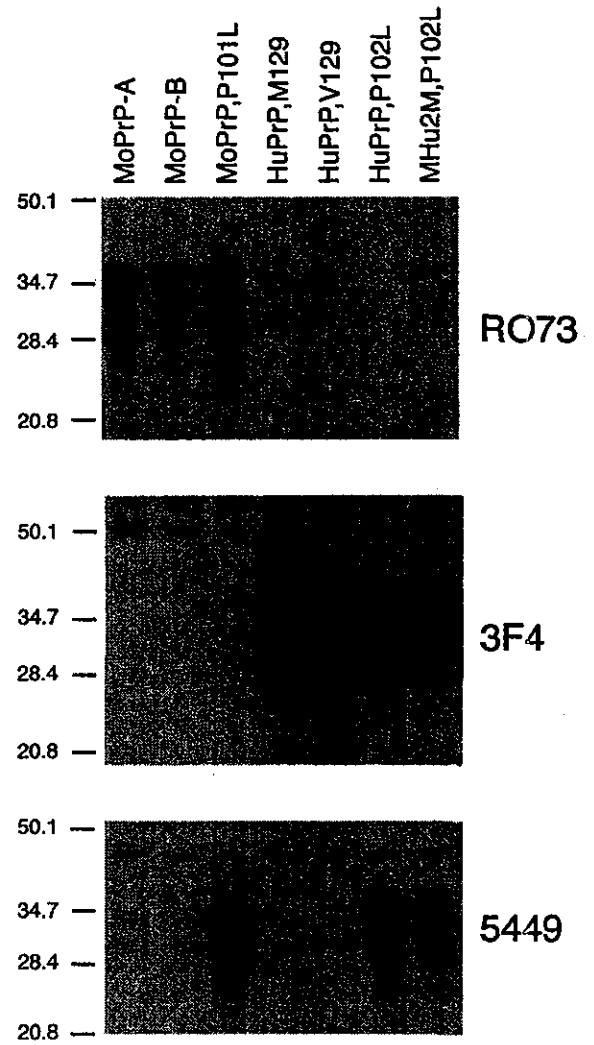

FIG. 1. Selective immunoreactivity of rabbit polyclonal antiserum 5449 raised against the MoPrP(89-143,P101L) peptide with PrPs carrying the P101L mutation. Brain homogenates (20 μg of total protein per lane) from mice expressing wt MoPrP-A (FVB), wt MoPrP-B (ILn/J), MoPrP(P101L) [Tg(MoPrP,P101L)196/$Prnp^{0/0}$], HuPrP(M129) [Tg(HuPrP,M129)440/$Prnp^{0/0}$], HuPrP(V129) [Tg(HuPrP,V129)152/$Prnp^{0/0}$], HuPrP(P102L) [Tg(HuPrP,P102L)7/$Prnp^{0/0}$], and MHu2M(P102L) [Tg(MHu2M,P102L)69/$Prnp^{0/0}$] were processed. Western blots were developed using the anti-PrP(P101L) 5449 polyclonal antiserum, and for comparison, with the anti-PrP RO73 polyclonal antiserum and the 3F4 monoclonal antibody. The apparent molecular weights of the migrated fragments are shown in thousands.

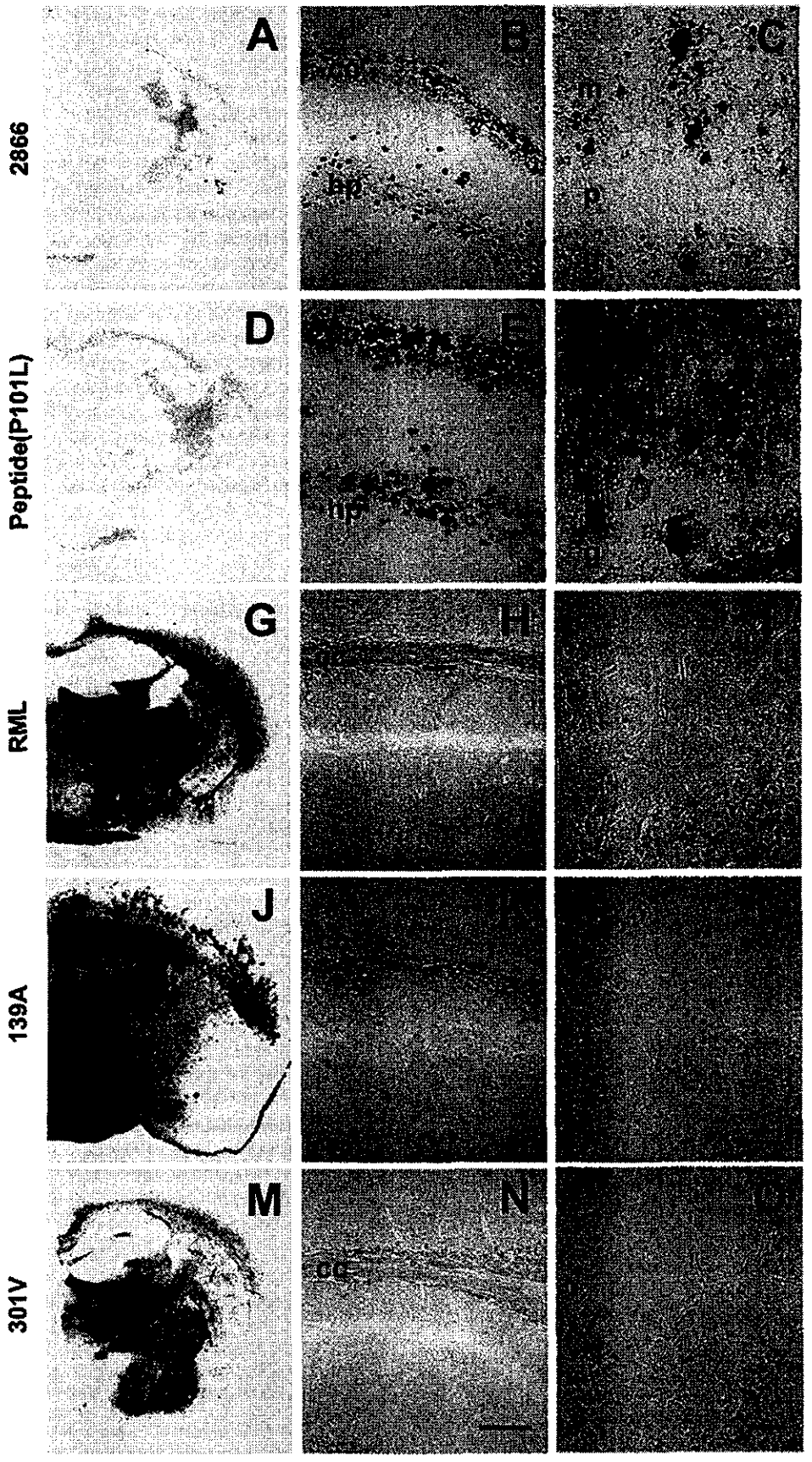
2866
Peptide(P101L)
RML
139A
301V
A
B
C
D
E
G
H
J
M
N
lp
m
p
cc

P101L) peptide showed numerous large (70 μm), multicentric, GSS-like plaques in the neocortex, hippocampus, corpus callosum, caudate nucleus, globus pallidus, and cerebellar cortex (Fig. 2E and F). All of these plaques stained with anti-PrP antibodies. Severe spongiform changes and astrocytic gliosis associated with the loss of granule cells and numerous immature, GSS-like amyloid plaques were found in the cerebellum.

Prion strains from wt mice. Tg196 mice were susceptible to prion strains isolated in wt mice. RML and 139A strains were isolated from sheep with naturally occurring scrapie and passaged in $Prnp^{a/a}$ mice. In CD-1 ($Prnp^{a/a}$) mice, the incubation periods for RML and 139A prions were ~130 and ~145 days, respectively. When RML and 139A prions were inoculated into Tg196 mice, prolonged incubation periods of ~230 and ~425 days, respectively, were observed (Table 2); on second passage, the incubation times shortened to ~180 days and ~190 days, respectively. 301V prions were isolated from cattle with BSE by passage in $Prnp^{b/b}$ mice. When 301V prions were transmitted from $Prnp^{b/b}$ mice to Tg196 mice, incubation periods of ~120 days and ~115 days were observed on first and second passage, respectively. 301V prions have similar incubation periods in $Prnp^{b/b}$ and Tg196 mice but produce incubation periods of ~230 days in CD-1 mice.

These findings suggest that the P101L mutation creates a transmission barrier for propagation of the RML and 139A prion strains previously passaged in $Prnp^{a/a}$ mice. In contrast, the mutation poses no transmission barrier for 301V prions previously passaged in $Prnp^{b/b}$ mice. Taken together, our findings argue that the P101L mutation has an effect on incubation times similar to that of the L108F and T189V substitutions encoded in mouse $Prnp^{b}$ (49).

Intracerebral inoculation of Tg196 mice with the RML, 139A, and 301V prions resulted in neuropathological changes typical of experimental scrapie. The accumulation of $rPrP^{Sc}$ was evident using the histoblot method (Fig. 2G, J, and M) and vacuolation of the gray matter localized with sites of PrP^{Sc} accumulation (data not shown). Small (25 μm), subcallosal PrP plaques were also present in the brains of RML- and 139A-inoculated animals (Fig. 2H to I, K to L, and N to O). No plaques were found in the cerebella of mice inoculated with any of these three prion strains (Figs. 2I, L, and O).

Histoblotting revealed that each of the three prion strains produced a unique distribution of $rPrP^{Sc}$ in the gray and/or white matter (Fig. 2G, J, and M). For example, 139A prions produced intense PrP^{Sc} immunostaining in the hippocampus, but inoculation with RML and 301V prions did not produce PrP^{Sc} deposits in this region. Inoculation with RML prions resulted in a mild degree of vacuolation in layers IV through VI of the neocortex (data not shown) that correlated well with the medium-intensity immunostaining for PrP^{Sc} confined to the inner half of the neocortex (Fig. 2G). In animals inoculated with the 301V strain, immunostaining was not observed in the neocortex (Fig. 2M) and vacuolation was not detected (data not shown).

Biochemical detection of MoPrP(P101L) conformers. Earlier attempts using PK digestion for prolonged durations failed to identify altered forms of MoPrP(P101L) that feature in neurodegeneration. Therefore, we employed two new approaches. First, we took advantage of the ability of PTA to differentially precipitate PrP^{Sc} while leaving PrP^{C} in the supernatant fraction. Second, we employed alternative conditions for PK digestions by lowering the temperature to 4°C, a condition employed previously to demonstrate alterative forms that mutant PrPs can adopt (25). The protease resistance of MoPrP(P101L) conformers was probed using two different protocols: (i) digestion with 25 μg of PK/ml for 1 h at 37°C and (ii) digestion with 250 μg of PK/ml for 1 h at 4°C. In previous studies, we designated the latter protocol using digestion at 4°C as "mild PK" to distinguish it from the "harsh PK" protocol with digestion at 37°C (25). In the interest of clarity, here we designate digestion at 4°C as "cold PK" and simply refer to digestion at 37°C as "PK" (Table 1).

As previously described, $rPrP^{Sc}$(P101L) was undetectable in the brains of spontaneously ill Tg2886 or ill Tg196 mice after inoculation with mouse GSS(P101L) prions (27, 28, 47). Similar results were obtained with Tg196 mice inoculated with the β-rich MoPrP(89-143,P101L) peptide and in subsequent passages (Fig. 3F) (29). Low levels of $rPrP^{Sc}$(P101L) were detected in spontaneously ill Tg2866 mice only when samples were concentrated by ultracentrifugation (Fig. 3C). These low levels of $rPrP^{Sc}$(P101L) in brain homogenates from Tg mice infected with GSS(P101L) prions or the β-rich MoPrP(89-143,P101L) peptide contrast with the high levels of $rPrP^{Sc}$(P101L) in Tg196 mice inoculated with RML, 139A, or 301V prions (Fig. 3C and data not shown).

Traces of PTA-precipitable PrP were found in uninoculated, age-matched, control Tg196 and Tg(MoPrP-A)4053/$Prnp^{0/0}$ mice (Fig. 3B). In contrast, the PTA-precipitable PrP fraction was severalfold greater in the brains of spontaneously ill Tg2866 mice and in Tg196 mice inoculated with brain homogenates from spontaneously ill Tg2866 mice.

In the brains of spontaneously ill Tg2866 mice, high levels of a PrP^{Sc} fragment migrating to 22 to 24 kDa on Western blots was detected by cold PK digestion; PrP 22-24 is the cold PK-resistant fragment of $sPrP^{Sc}$(P101L) (Table 1). PrP 22-24 was also found in Tg196 mice following inoculation with mouse GSS(P101L) prions or with the β-rich MoPrP(89-143,P101L) peptide after first and second passages (Fig. 3D to F). The cold PK-resistant signal was stronger after PTA precipitation. Normal, age-matched Tg196 mice (~350 days of age) and Tg4053

FIG. 2. GSS-like neuropathological features in the absence of PK-resistant PrP^{Sc} in spontaneous and synthetic peptide-induced prion disease in Tg mice expressing the MoPrP(P101L) allele. The analyzed brains are from Tg(MoPrP,P101L)196/$Prnp^{0/0}$ mice inoculated with prions from spontaneously ill Tg(MoPrP,P101L)2866/$Prnp^{0/0}$ mice (A, B, and C), β-rich MoPrP(89–143,P101L) peptide (D, E, and F), or for comparison, with RML (G, H, and I), 139A (J, K, and L), or 301V (M, N, and O) prions. Distribution of $rPrP^{Sc}$ was determined by histoblotting (A, D, G, J, and M), and PrP-immunoreactive plaques were detected by hydrolytic autoclaving in the hippocampus (B, E, H, K, and N) and cerebellum (C, F, I, L, and O). Abbreviations: cc, corpus callosum; g, granule cell layer; hp, stratum radiatum of the CA1 region of the hippocampus; m, molecular layer; p, Purkinje cell layer. The bar in panel N represents 100 μm and applies to panels B, E, H, and K; The bar in panel O represents 30 μm and applies to panels C, F, I, and L.

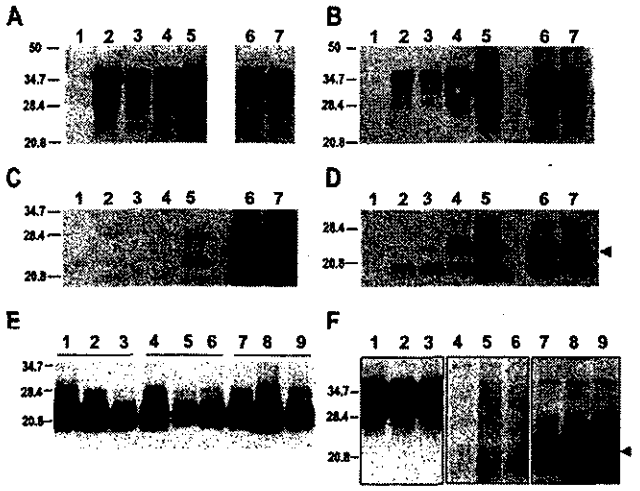

FIG. 3. Serial passage of aberrant PrP conformers in Tg(MoPrP, P101L) mice, detected by selective PTA precipitation and cold PK treatment. The 22- to 24-kDa PrP fragment (arrowheads) was found exclusively in Tg196 mice following inoculation with mouse GSS(P101L) prions or the β-rich MoPrP(89-143,P101L) peptide after both first and second passages. (A to D) Brain homogenates from uninoculated $Prnp^{0/0}$ mice (lane 1), Tg(MoPrP-A)4053/$Prnp^{0/0}$ mice (lane 2), uninoculated Tg(MoPrP,P101L)196/$Prnp^{0/0}$ mice (lane 3), Tg196 mice inoculated with brain homogenates from ill Tg2866 mice (lane 4), spontaneously ill Tg2866 mice (lane 5), Tg196 mice inoculated with RML prions (lane 6), or Tg196 mice inoculated with 301V prions (lane 7) are shown. Brain homogenates were untreated (A), precipitated with PTA (B), PK digested and subjected to ultracentrifugation (C), or subjected to cold PK digestion and precipitated with PTA (D). (E) Brain homogenates subjected to cold PK digestion and PTA precipitation from spontaneously ill Tg2866 mice (lanes 1 to 3), Tg196 mice inoculated with brain homogenates of diseased Tg2866 mice (lanes 4 to 6), or second passage of Tg2866 brain homogenates in Tg196 mice (lanes 7 to 9). (F) Brain homogenates from Tg196 mice inoculated with brain homogenates from ill Tg2866 mice (lanes 1, 4, and 7), β-rich MoPrP(89-134,P101L) peptide (lanes 2, 5, and 8), or second passage of MoPrP(89-134,P101L) peptide into Tg196 mice (lanes 3, 6, and 9). Samples were untreated (lanes 1 to 3), PK digested and ultracentrifuged (lanes 4 to 6), or subjected to cold PK digestion and PTA precipitation (lanes 7 to 9). Blots were developed using anti-PrP RO73 (A to D) or anti-PrP(P101L) 5449 polyclonal antisera raised against a random-coil MoPrP(89–143,P101L) peptide (E and F). The apparent molecular weights of the migrated fragments are shown in thousands.

mice (~140 days of age) did not display PrP 22-24 (Fig. 3D). A shorter PrP fragment of ~19 kDa was detected using the cold PK assay in all mice when blots were stained with anti-PrP RO73 polyclonal antiserum (Fig. 3D) but not when using the 5449 antiserum, which reacts only with residues 89 to 143 of MoPrP(P101L) (Fig. 3E and F). The 19-kDa fragment probably corresponds to the C-terminal portion of PrP.

Transmission of mouse GSS(P101L) prions. We measured prion infectivity in the brains of uninoculated Tg2866 mice after they spontaneously developed CNS dysfunction at ~130 days of age. Brain homogenates from Tg2866 mice were subjected to PTA precipitation alone or in combination with PK digestion before bioassay in Tg196 mice (Table 3). Untreated brain homogenates from Tg2866 mice produced disease in Tg196 mice at ~305 days, while PTA precipitation followed by PK digestion reduced the incubation time to ~225 days. This ~80-day reduction in the incubation time is highly significant, with a P value of <0.0014 (analysis of variance), arguing that the prions in the brains of Tg2866 mice are resistant to PK digestion.

Similar results were obtained when brain extracts were prepared from Tg196 mice previously inoculated with Tg2866 brain homogenates. The untreated homogenates from the Tg196(2866) mice produced disease in inoculated Tg196 mice after ~350 days, while PTA precipitation followed by PK digestion reduced the incubation time to ~280 days (Table 3). This ~70-day reduction in the incubation time is highly significant, with a P value of < 0.0005 (analysis of variance), arguing that the prions in the brains of Tg196(2866) mice are also resistant to PK digestion.

In contrast to the studies with inocula derived from the brains of Tg2866 mice, untreated inocula from the brains of neurologically normal Tg196 mice at ~300 days of age produced disease in six of seven Tg196 mice after ~480 days (Table 3). Moreover, inocula subjected to PTA precipitation followed by PK digestion produced disease at ~480 days but only in one of nine Tg196 mice. When 301V prions were inoculated into Tg196 mice, the incubation period was ~145 days, which was reduced by ~15 days when the inoculum was first subjected to PTA precipitation and PK digestion; this 10% reduction in incubation time is statistically insignificant. The 301V prions were initially isolated from BSE brain by passage in VM mice harboring the $Prnp^{b/b}$ alleles and subsequently passaged in B6.1 mice also carrying $Prnp^{b/b}$ alleles, with an incubation time of ~115 days (Table 2). On subsequent passages in Tg196 mice, the incubation times ranged from 115 to 145 days (Tables 2 and 3).

Age-dependent accumulation of prions in Tg2866 mice. We measured prion infectivity in the brains of Tg2866 mice by sacrificing the mice at various ages and inoculating their brain extracts into Tg196 mice. BH from Tg2866 mice sacrificed either at birth or at 56 days of age contained no detectable levels of prion infectivity, based on bioassays in Tg196 mice (Fig. 4E). Low levels of infectivity were found in 84-day-old Tg2866 mice: brain extracts from these mice inoculated into Tg196 mice induced disease in two of nine animals at ~440 days postinoculation (Fig. 4E). Brain extracts from 112-day-old Tg2866 mice produced disease after ~350 days of incubation in 9 of 10 animals. When Tg2866 mice developed signs of CNS dysfunction at ~130 days, the mice were sacrificed and their BH were inoculated into Tg196 mice. All eight inoculated Tg196 mice developed disease, with a mean incubation period of ~260 days (Fig. 4E). No infectivity was detected in the brains of age-matched, control Tg4053 mice (130 days of age), based on bioassays in Tg196 mice (0 of 10 animals, >500 days); Tg4053 mice express wt MoPrP at levels similar to mutant MoPrP(P101L) expressed in Tg2866 mice. This progressive shortening of incubation periods is consistent with an increase in the titer of infectious prions in the brains of Tg2866 mice as they age.

The progressive accumulation of infectious GSS(P101L) prions in Tg2866 mice as they aged correlated with the appearance of $sPrP^{Sc}$(P101L). PrP 22-24 was detected at 112 days and ~130 days using the cold PK digestion protocol (Fig. 4C). Curiously, Tg2866 mice showed a transient postnatal upregulation of mutant MoPrP(P101L) expression between 14 and 56 days of age (Fig. 4A). Levels of $sPrP^{Sc}$(P101L) were highest in

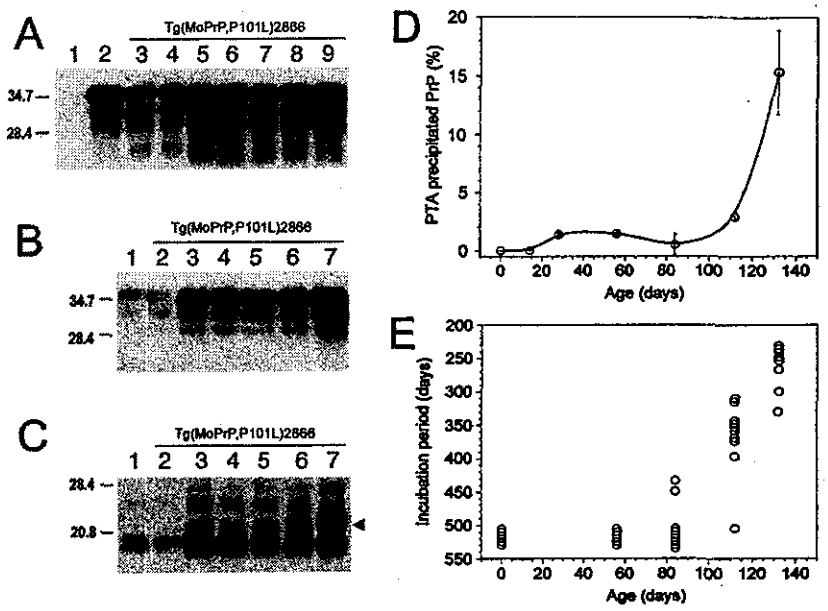

FIG. 4. Progressive accumulation of abnormal MoPrP(P101L) conformers (A to D) correlates with the accumulation of infectious prions (E) as a function of age in Tg(MoPrP,P101L)2866/$Prnp^{0/0}$ mice. Presymptomatic animals were sacrificed at birth, at 14 days, 28 days, 56 days, 84 days, or 112 days of age or at ~132 days (when diagnosed with CNS dysfunction). Blots were developed using the RO73 polyclonal antibody. The apparent molecular weights of the migrated fragments are shown in thousands. (A) Untreated brain homogenates from $Prnp^{0/0}$ mice (lane 1), Tg4053 mice (lane 2), or Tg2866 mice (lanes 3 to 9) sacrificed at birth (lane 3), 14 days (lane 4), 28 days (lane 5), 56 days (lane 6), 84 days (lane 7), 112 days (lane 8), or ~132 days (lane 9). (B) Brain homogenates from Tg4053 mice (lane 1), Tg2866 mice sacrificed at 14 days (lane 2), 28 days (lane 3), 56 days (lane 4), 84 days (lane 5), 112 days (lane 6), or ~132 days (lane 7). Samples were precipitated with PTA prior to immunoblotting. (C) Brain homogenates subjected to cold PK digestion followed by PTA precipitation. Lane assignments are as described for panel B. The presence of a 22-kDa to 24-kDa PrP fragment specific to infectious GSS prions is indicated by the arrowhead. (D) The accumulation of abnormal PrP conformers in the brains of aging Tg(MoPrP,P101L)2866/$Prnp^{0/0}$ mice was quantified using the CDI with the RO73 antiserum and a secondary Eu-labeled anti-rabbit polyclonal antibody. (E) The same brain homogenates from aging Tg(MoPrP,P101L)2866/$Prnp^{0/0}$ mice used in the CDI were inoculated into Tg(MoPrP,P101L)196/$Prnp^{0/0}$ mice to measure incubation times, which are inversely proportional to the prion titer (38). Animals that did not display signs of neurological dysfunction were sacrificed after 500 days.

Tg2866 mice at ~130 days of age, when these mice developed CNS disease (Fig. 4B).

GSS(P102L) prions in human patients and Tg mice. We assessed whether the progressive accumulation of abnormal PrP conformers observed in Tg2866 mice applies to GSS patients and to Tg mice expressing the MHu2M transgene with the corresponding P102L mutation, designated Tg(MHu2M,P102L)69/$Prnp^{0/0}$ mice. Tg69 mice developed CNS disease spontaneously at ~400 days of age; however, when Tg69 mice were inoculated with brain extracts from patients who died of GSS, they developed disease ~170 days after inoculation.

Brain samples from Tg69 mice and from patients with GSS were subjected to PTA precipitation alone or after cold PK digestion. These brain samples displayed increased levels of $sHuPrP^{Sc}$(P102L) compared to untreated samples (Fig. 5A, B, and D). Mutant HuPrP 22-24 was found in Tg69 mice at 200 days of age (Fig. 5D) and at much higher levels in spontaneously ill Tg69 mice at ~360 days of age (Fig. 5F and H).

Conformation-dependent immunoassay. The development of the CDI permitted measurement of both $rPrP^{Sc}$ and $sPrP^{Sc}$ (39). We used the CDI to measure the relative ratios of $rPrP^{Sc}$ and $sPrP^{Sc}$ in the brains of Tg196 and Tg2866 mice (Table 1). No $sPrP^{Sc}$(P101L) was detectable in the brains of uninoculated Tg196 mice, while $sPrP^{Sc}$(P101L) comprised ~15% of total PrP in spontaneously ill Tg2866 mice (Fig. 6A). As noted above, $sPrP^{Sc}$(P101L) is measured by cold PK digestion followed by PTA precipitation. In the brains of Tg196 mice inoculated with prions from Tg2866 mice, $sPrP^{Sc}$(P101L) accounted for ~20% of total PrP. In the brains of Tg196 mice inoculated with prions derived from sheep (RML) or cattle (301V), $sPrP^{Sc}$(P101L) comprised ~25% of total PrP. PK digestion followed by ultracentrifugation showed that $rPrP^{Sc}$ (P101L) was undetectable in the brains of uninoculated Tg196 mice. In contrast, $rPrP^{Sc}$(P101L) represented ~5% of the total PrP in the brains of spontaneously ill Tg2866 mice (Fig. 6A). In Tg196 mice inoculated with prions from Tg2866 mice, ~10% of total PrP was PK resistant; in Tg196 mice inoculated with either RML or 301V prions, ~20% of the total PrP was PK resistant.

When $rPrP^{Sc}$(P101L) was plotted as a function of the ratio of denatured (D) to native (N) PrP^{Sc}, as measured by time-resolved fluorescence spectrometry (Fig. 6B), the PrP^{Sc} (P101L) conformers found in the brains of spontaneously ill Tg2866 mice were distinct from those found in Tg196 mice inoculated with RML or 301V prions. The PrP^{Sc}(P101L) conformers found in spontaneously ill Tg2866 mice were indistinguishable from those found in the three groups of mice: (i) Tg196 mice inoculated with the MoPrP(89-143,P101L) peptide; (ii) Tg196 mice inoculated with brain extracts from ill Tg196 mice that were inoculated with the MoPrP(89-143, P101L) peptide; and (iii) Tg196 inoculated with brain extracts

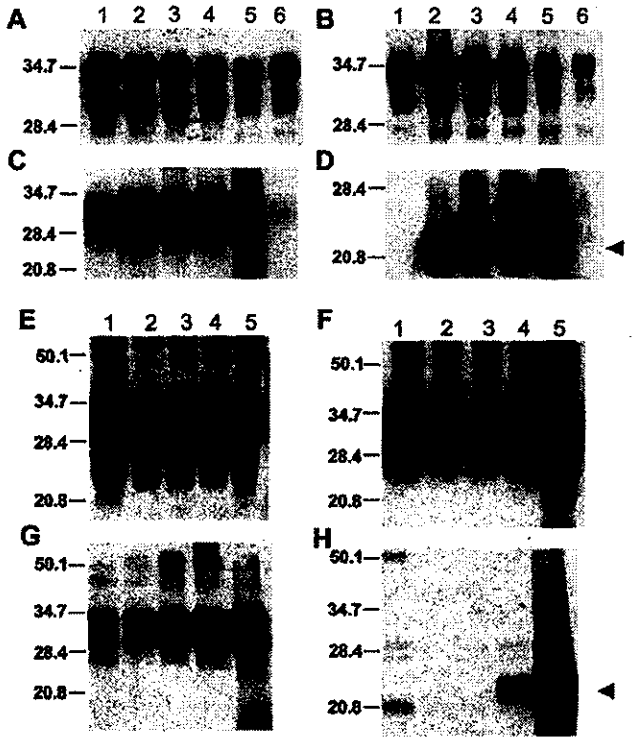

FIG. 5. Aberrant HuPrP(P102L) conformers present in the brains of GSS patients and GSS-inoculated Tg mice (A to D) are indistinguishable from those that progressively accumulate in spontaneously ill chimeric Tg(MHu2M,P102L) mice (E to H). Samples were developed using the 3F4 monoclonal antibody. The apparent molecular weights of migrated fragments are shown in thousands. The presence of a 22-kDa to 24-kDa PrP fragment specific to GSS prions is indicated by the arrowheads. (A to D) Brain homogenates from spontaneously ill Tg(MHu2M,P102L)69/*Prnp*$^{0/0}$ mice (lane 2), Tg(MHu2M,P102L) mice inoculated with homogenates from GSS patients expressing either Val (lane 3) or Met (lane 4) at codon 129, and a GSS(P102L,M129) patient (lane 5). As controls, homogenates from an age-matched, healthy Tg(MHu2M)*Prnp*$^{0/0}$ mouse (lane 1) and normal human brain (lane 6) are shown. (E to H) Brain homogenates from spontaneously ill Tg69 mice sacrificed at 50 days (lane 2), 100 days (lane 3), 200 days (lane 4), ~360 days (lane 5), when the mice became ill, demonstrate the accumulation of PrP^{Sc} conformers that are similar to those observed in GSS patients. As a control, homogenate from a healthy, age-matched Tg(MHu2M)*Prnp*$^{0/0}$ mouse (lane 1) is shown. Samples were untreated (A and E), precipitated with PTA (B and F), digested with PK followed by ultracentrifugation (C and G), or subjected to cold PK digestion followed by PTA precipitation (D and H).

from ill Tg2866 mice. These findings support the contention that the GSS prions either arising spontaneously in Tg2866 mice or induced in Tg196 mice by the 55-mer MoPrP(89-143, P101L) peptide are distinct from prion strains derived from sheep with scrapie (RML) and cattle with BSE (301V).

DISCUSSION

The results reported here permit, for the first time, biophysical correlations with prion infectivity generated in mice expressing MoPrP(P101L) transgenes. Although the first Tg mice expressing MoPrP(P101L) were constructed more than a decade ago (26, 27, 47), the lack of biophysically detectable alterations in mutant MoPrP(P101L) has compromised the utility of this model system, until now. Selective precipitation of PrP^{Sc}(P101L) with PTA in combination with cold PK digestion provides a new tool for dissecting the molecular mechanisms of inherited prion diseases. In addition, the results presented here coupled with an earlier report (29) argue that MoPrP(89-143, P101L) in a β-rich conformation triggers the generation of de novo GSS prions; indeed, our findings provide compelling evidence that this 55-mer mutant peptide folded into a β-rich structure is a synthetic prion.

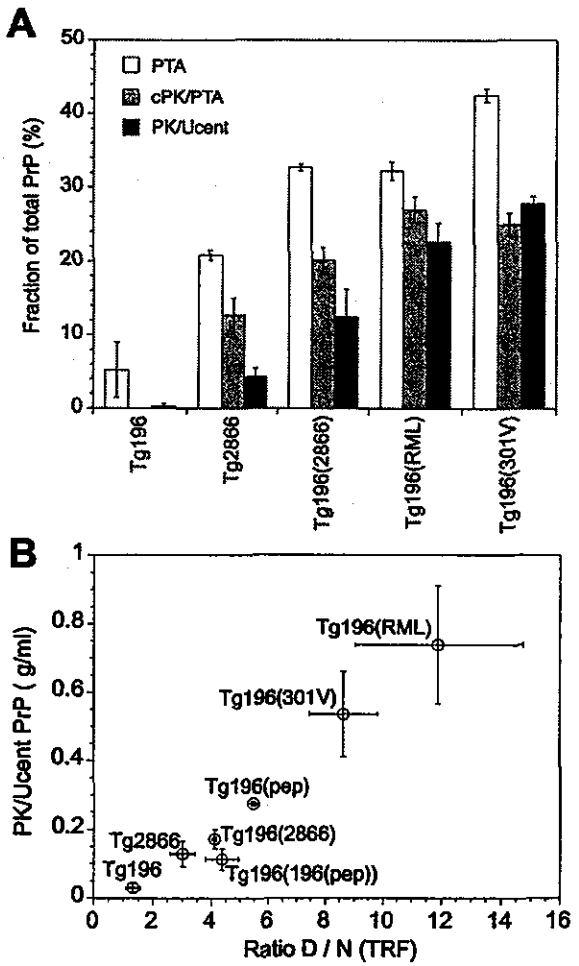

FIG. 6. Differential proteolytic resistance of aberrant, distinct PrP conformers in the brains of Tg(MoPrP,P101L) mice detected by the CDI. (A) Brain homogenates from spontaneously ill Tg(MoPrP, P101L)2866/*Prnp*$^{0/0}$ mice and Tg(MoPrP,P101L)196/*Prnp*$^{0/0}$ mice inoculated with RML prions, 301V prions, or GSS(P101L) prions from ill Tg2866 mice. Controls were age matched, uninoculated Tg mice. Samples were either left untreated (total PrP content), PTA precipitated, digested with cold PK followed by PTA precipitation (cPK/PTA), or digested with PK followed by ultracentrifugation (PK/Ucent). Results are shown as the fraction of total PrP recovered after each treatment. (B) Amount of $rPrP^{Sc}$ recovered after ultracentrifugation plotted as a function of the amount of antibody bound to the denatured and native forms of PrP (D:N ratio). Samples were obtained from the same mice depicted in panel A, in addition to Tg(MoPrP,P101L)196/*Prnp*$^{0/0}$ mice inoculated with the β-rich MoPrP(89-143,P101L) peptide on first [Tg196(pep)] and second [Tg196(196(pep))] passage. Data points and bars represent the means ± standard errors of the mean obtained from three independent measurements.

Synthetic prions. In an effort to construct a synthetic prion, we chose to focus our efforts on a genetic form of prion disease in order to bias the folding of PrP into a PrP^{Sc} isoform. Multiple attempts to generate prion infectivity from refolded recombinant PrPs have been unsuccessful to date (5–7). Since GSS(P102L) is the only inherited prion disease that has been successfully modeled in mice with respect to generating infectivity de novo, we chose to exploit the P102L mutation. To produce a synthetic prion, we constructed the 55-mer MoPrP (89-143,P101L) peptide using solid-phase peptide synthesis. When folded into a β-rich conformation, MoPrP(89-143, P101L) induced prion disease in Tg196 mice (Table 2) (29). The same peptide did not induce disease when it was not folded into a β-rich conformation. That the peptide must be in β-rich structure and the host must express MoPrP(P101L) in order to induce disease underscores the conformational specificity of prion propagation.

We report here that the disease induced in Tg196 mice by the β-rich MoPrP(89-143,P101L) peptide can be serially transmitted to Tg196 mice with an incubation time of ~350 days (Table 2). The presence of large multicentric plaques, which deposit in the neocortex, caudate nucleus, corpus callosum, hippocampus, and cerebellar cortex, together with focal vacuolar changes, corroborate the distinct characteristics of these GSS prions. From these experimental findings and those presented previously, we argue that the mutant 55-mer, β-rich peptide fulfills all of the criteria required for designation as a synthetic prion.

The neuropathologic changes characteristic of humans carrying the GSS(P102L) mutation, including large, multicentric plaques that stain with anti-PrP antibodies, are preserved in Tg(MoPrP,P101L) mice that develop prion disease spontaneously as well as in those that develop disease after inoculation with GSS prions or with the mutant 55-mer β-rich peptide. In contrast, when human GSS(P102L) prions are transmitted to nonhuman primates or non-Tg mice, these GSS-type plaques are rarely found (1, 32, 46). This distinction argues that the P→L substitution imposes a conformational constraint on host PrP^{C} that is required to preserve the disease characteristics of GSS.

It is noteworthy that polypeptides comprising the N domain of the yeast Sup35 protein have been expressed in *Escherichia coli* and folded into a β-rich conformation (3, 44). Such polypeptides readily polymerize into amyloid, which has been transferred into [PSI^{-}] *Saccharomyces cerevisiae* that in turn becomes [PSI^{+}], the prion state. As with the mutant 55-mer, β-rich peptide studies reported previously (29), these experiments with yeast argue for the production of a synthetic prion and contend that prions are composed only of protein, in accord with a wealth of other data (36).

Prion strains. Based on differences in resistance to limited proteolysis, two groups of prion strains can be distinguished: (i) those with low levels and (ii) those with high levels of $rPrP^{Sc}$ (P101L). Strains with low levels of $rPrP^{Sc}$(P101L) are formed spontaneously in Tg2866 mice and are formed in Tg196 mice after inoculation with either GSS(P101L) prions or the mutant 55-mer β-rich synthetic peptide. Prion strains with high levels of $rPrP^{Sc}$(P101L) were formed in Tg196 mice after inoculation with RML, 139A, or 301V prions. This last group of prion strains can be subdivided into two groups based on their incubation times in Tg196 mice: RML and 139A prions produce long incubation times, whereas 301V prions result in short incubation times. The P101L substitution in Tg196 mice introduced a transmission barrier and lengthened the incubation periods of RML and 139A prions (~180 days) compared to those observed in wt $Prnp^{a/a}$ mice (~130 days). In contrast, the replication of 301V prions in Tg196 mice did not encounter a transmission barrier, with incubation periods of ~125 days, similar to those found in $Prnp^{b/b}$ B6.I mice (Tables 2 and 3) (12). Since the phenomenon of transmission barriers induced by mutations was observed also in yeast prion [PSI^{+}], the mechanism appears to be a general paradigm for all prions regardless of the host or strain (17).

Conformational characteristics of PrP^{Sc}. The wide use of limited proteolysis to detect PrP 27-30 created the expectation that Tg(MoPrP,P101L) mice spontaneously developing CNS disease should possess readily detectable levels of mutant PrP 27-30 (15, 16). When PrP 27-30 was not found after limited PK digestion at 37°C, the modeling of GSS in Tg mice was thought to be unconvincing and prompted some investigators to doubt the interpretation of genetic linkage studies of humans carrying pathological mutations in the PrP gene.

In the studies reported here, we demonstrate that PrP^{Sc} conformers accumulate in the brains of Tg(MoPrP,P101L) mice that develop prion disease spontaneously as well as those that were inoculated with either GSS prions or the mutant 55-mer β-rich peptide. By modifying the conditions for limited proteolysis, we consistently demonstrated high levels of a disease-specific $sPrP^{Sc}$(P101L) conformer that generated PrP 22-24 upon cold PK digestion that was absent from the brains of wt mice (Table 1). Moreover, $sPrP^{Sc}$(P101L) accumulated in the brains of Tg2866 mice as a function of age and reached maximal levels when the mice displayed neurologic signs of prion disease (Fig. 5).

In the studies described here, PrP^{Sc}(P101L) adopted one conformation that was most readily detectable only after cold PK digestion and another conformation that was assayed by PK digestion at 37°C. Cold PK digestion demonstrated the presence of $sPrP^{Sc}$(P101L) in the brains of Tg2866 mice that develop prion disease spontaneously as well as of Tg196 mice that were inoculated with either GSS prions or the mutant 55-mer β-rich peptide (Fig. 3 to 5). PK digestion at 37°C was used to demonstrate $rPrP^{Sc}$(P101L) in the brains of Tg196 mice inoculated with prion strains derived from sheep with scrapie (RML and 139A prions) or cattle with BSE (301V prions) (Fig. 3C).

Defining the conformations of PrP^{Sc}(P101L) and wt PrP^{Sc} molecules promises to be difficult, since both are quite insoluble. Currently, the best approach to elucidating the structural features of wt PrP^{Sc} has been by electron crystallography of two-dimensional crystals (50). From the PK digestion studies of RML, 139A, and 301V prions propagated in Tg196 mice, it is reasonable to argue that $rPrP^{Sc}$(P101L) and wt $rPrP^{Sc}$ probably have similar structures. It is less clear how $sPrP^{Sc}$(P101L) in the brains of ill Tg2866 and Tg196 mice is related to wt $sPrP^{Sc}$. Assessing this relationship is difficult because no procedure has been developed to separate wt $sPrP^{Sc}$ from wt $rPrP^{Sc}$. Using the CDI, wt $sPrP^{Sc}$ can be calculated by subtracting PrP 27-30 from total PrP^{Sc}.

When the brains of Tg2866 mice were subjected to PK

digestion before or after PTA precipitation and inoculated into mice, the resulting incubation times were shorter than those obtained with untreated brain homogenates (Table 3), presumably reflecting increased titers due to the concentration of prions by selective PTA precipitation. Moreover, these results indicate that prion infectivity in the brains of Tg2866 mice is resistant to limited digestion with 25 μg of PK/ml for 1 h at 37°C. Similar resistance to proteolytic digestion was observed in the brains of Tg196 mice inoculated with either Tg2866 brain homogenates or 301V prions. The characteristics of different PrP isoforms are summarized in Table 1.

Mechanisms of neurodegeneration. Although there are many examples of modified PrP^C molecules, only PrP(P101L) has been shown to initiate an experimental prion disease that is transmissible. In studies using Tg mice, the expression of the D178N mutation did not produce neurologic deficits. The E200K and A117V mutations produced neurologic diseases, but brains from Tg mice carrying these mutations failed to transmit disease on passage in wt or isogenic hosts (24; P. Tremblay et al., unpublished observations). Similarly, the expression of a PrP transgene harboring an octapeptide repeat expansion from 5 to 14 repeats has been shown to initiate a spontaneous neurodegenerative condition similar to that observed in humans with prion disease (18, 19), but despite the accumulation of insoluble PrP conformers displaying low levels of protease resistance, the transmissibility of this disease has yet to be demonstrated. Expression of various designer mutations that led to the generation of PrP^C molecules with a transmembrane topology produced neurologic deficits correlating to the synthesis of topologically distinct, transmembrane PrP molecules (24, 25); again, attempts to transmit these diseases have failed (R. S. Hegde et al., unpublished observations). The general model emerging from all those experiments suggests that there are two probably independent misfolding pathways of mutant PrP: one leading to accumulation of misfolded conformers causing neurodegeneration and the other pathway leading to the accumulation of conformers that are infectious; whether the infectious conformers are also those that cause neurodegeneration remains to be established.

New directions in prion research. The discoveries reported here describe relatively crude biophysical correlations with prion infectivity generated in mice expressing MoPrP(P101L) transgenes. More detailed analyses might prove to be relevant in dissecting the mechanism of prion formation in the inherited prion diseases. The MoPrP(P101L) transgene has been unexpectedly useful in the study of prion strains. Coupled with new approaches using PTA precipitation and cold PK digestion, Tg mice expressing MoPrP(P101L) may increase our understanding of the mechanism by which prions are formed spontaneously as well as the structural features that encipher strain-specific information.

ACKNOWLEDGMENTS

This work was supported by grants from the National Institutes of Health (AG02132 and AG010770) and by a gift from the Leila Y. and G. Harold Mathers Charitable Foundation.

We thank the Hunter's Point Animal Facility.

REFERENCES

1. **Baker, H. F., L. W. Duchen, J. M. Jacobs, and R. M. Ridley.** 1990. Spongiform encephalopathy transmitted experimentally from Creutzfeldt-Jakob and familial Gerstmann-Sträussler-Scheinker diseases. Brain 113:1891–1909.
2. **Baker, H. F., R. M. Ridley, and T. J. Crow.** 1985. Experimental transmission of an autosomal dominant spongiform encephalopathy: does the infectious agent originate in the human genome? Br. Med. J. 291:299–302.
3. **Balbirnie, M., R. Grothe, and D. S. Eisenberg.** 2001. An amyloid-forming peptide from the yeast prion Sup35 reveals a dehydrated β-sheet structure for amyloid. Proc. Natl. Acad. Sci. USA 98:2375–2380.
4. **Barry, R. A., and S. B. Prusiner.** 1986. Monoclonal antibodies to the cellular and scrapie prion proteins. J. Infect. Dis. 154:518–521.
5. **Baskakov, I. V., C. Aagaard, L. Mehlhorn, H. Wille, D. Groth, M. A. Baldwin, S. B. Prusiner, and F. E. Cohen.** 2000. Self-assembly of recombinant prion protein of 106 residues. Biochemistry 39:2792–2804.
6. **Baskakov, I. V., G. Legname, M. A. Baldwin, S. B. Prusiner, and F. E. Cohen.** 2002. Pathway complexity of prion protein assembly into amyloid. J. Biol. Chem. 277:21140–21148.
7. **Baskakov, I. V., G. Legname, S. B. Prusiner, and F. E. Cohen.** 2001. Folding of prion protein to its native α-helical conformation is under kinetic control. J. Biol. Chem. 276:19687–19690.
8. **Bolton, D. C., M. P. McKinley, and S. B. Prusiner.** 1982. Identification of a protein that purifies with the scrapie prion. Science 218:1309–1311.
9. **Brown, P., C. J. Gibbs, Jr., P. Rodgers-Johnson, D. M. Asher, M. P. Sulima, A. Bacote, L. G. Goldfarb, and D. C. Gajdusek.** 1994. Human spongiform encephalopathy: the National Institutes of Health series of 300 cases of experimentally transmitted disease. Ann. Neurol. 35:513–529.
10. **Bruce, M., A. Chree, I. McConnell, J. Foster, G. Pearson, and H. Fraser.** 1994. Transmission of bovine spongiform encephalopathy and scrapie to mice: strain variation and the species barrier. Phil. Trans. R. Soc. Lond. B 343:405–411.
11. **Büeler, H., M. Fisher, Y. Lang, H. Bluethmann, H.-P. Lipp, S. J. DeArmond, S. B. Prusiner, M. Aguet, and C. Weissmann.** 1992. Normal development and behaviour of mice lacking the neuronal cell-surface PrP protein. Nature 356:577–582.
12. **Carlson, G. A., C. Ebeling, S.-L. Yang, G. Telling, M. Torchia, D. Groth, D. Westaway, S. J. DeArmond, and S. B. Prusiner.** 1994. Prion isolate specified allotypic interactions between the cellular and scrapie prion proteins in congenic and transgenic mice. Proc. Natl. Acad. Sci. USA 91:5690–5694.
13. **Carlson, G. A., D. T. Kingsbury, P. A. Goodman, S. Coleman, S. T. Marshall, S. DeArmond, D. Westaway, and S. B. Prusiner.** 1986. Linkage of prion protein and scrapie incubation time genes. Cell 46:503–511.
14. **Chandler, R. L.** 1961. Encephalopathy in mice produced by inoculation with scrapie brain material. Lancet i:1378–1379.
15. **Chesebro, B.** 1998. Prion diseases: BSE and prions: uncertainties about the agent. Science 279:42–43.
16. **Chesebro, B.** 1992. PrP and the scrapie agent. Nature 356:560.
17. **Chien, P., A. H. DePace, S. R. Collins, and J. S. Weissman.** 2003. Generation of prion transmission barriers by mutational control of amyloid conformations. Nature 424:948–951.
18. **Chiesa, R., B. Drisaldi, E. Quaglio, A. Migheli, P. Piccardo, B. Ghetti, and D. A. Harris.** 2000. Accumulation of protease-resistant prion protein (PrP) and apoptosis of cerebellar granule cells in transgenic mice expressing a PrP insertional mutation. Proc. Natl. Acad. Sci. USA 97:5574–5579.
19. **Chiesa, R., P. Piccardo, B. Ghetti, and D. A. Harris.** 1998. Neurological illness in transgenic mice expressing a prion protein with an insertional mutation. Neuron 21:1339–1351.
20. **DeArmond, S. J., and J. W. Ironside.** 1999. Neuropathology of prion diseases, p. 585–652. *In* S. B. Prusiner (ed.), Prion biology and diseases. Cold Spring Harbor Laboratory Press, Cold Spring Harbor, N.Y.
21. **Dickinson, A. G.** 1976. Scrapie in sheep and goats, p. 209–241. *In* R. H. Kimberlin (ed.), Slow virus diseases of animals and man. North-Holland Publishing, Amsterdam, The Netherlands.
22. **Fraser, H., M. E. Bruce, A. Chree, I. McConnell, and G. A. H. Wells.** 1992. Transmission of bovine spongiform encephalopathy and scrapie to mice. J. Gen. Virol. 73:1891–1897.
23. **Gambetti, P., R. B. Peterson, P. Parchi, S. G. Chen, S. Capellari, L. Goldfarb, R. Gabizon, P. Montagna, E. Lugaresi, P. Piccardo, and B. Ghetti.** 1999. Inherited prion diseases, p. 509–583. *In* S. B. Prusiner (ed.), Prion biology and diseases. Cold Spring Harbor Laboratory Press, Cold Spring Harbor, N.Y.
24. **Hegde, R. S., J. A. Mastrianni, M. R. Scott, K. A. DeFea, P. Tremblay, M. Torchia, S. J. DeArmond, S. B. Prusiner, and V. R. Lingappa.** 1998. A transmembrane form of the prion protein in neurodegenerative disease. Science 279:827–834.
25. **Hegde, R. S., P. Tremblay, D. Groth, S. B. Prusiner, and V. R. Lingappa.** 1999. Transmissible and genetic prion diseases share a common pathway of neurodegeneration. Nature 402:822–826.
26. **Hsiao, K., M. Scott, D. Foster, S. J. DeArmond, and S. B. Prusiner.** 1990. Towards a model of Gerstmann-Sträussler-Scheinker syndrome in transgenic mice. Soc. Neurosci. Abstr. 16(part 2):1138.
27. **Hsiao, K. K., D. Groth, M. Scott, S.-L. Yang, H. Serban, D. Rapp, D. Foster, M. Torchia, S. J. DeArmond, and S. B. Prusiner.** 1994. Serial transmission in rodents of neurodegeneration from transgenic mice expressing mutant prion protein. Proc. Natl. Acad. Sci. USA 91:9126–9130.
28. **Hsiao, K. K., M. Scott, D. Foster, D. F. Groth, S. J. DeArmond, and S. B.**

Prusiner. 1990. Spontaneous neurodegeneration in transgenic mice with mutant prion protein. Science 250:1587–1590.
29. Kaneko, K., H. L. Ball, H. Wille, H. Zhang, D. Groth, M. Torchia, P. Tremblay, J. Safar, S. B. Prusiner, S. J. DeArmond, M. A. Baldwin, and F. E. Cohen. 2000. A synthetic peptide initiates Gerstmann-Sträussler-Scheinker (GSS) disease in transgenic mice. J. Mol. Biol. 295:997–1007.
30. Kascsak, R. J., R. Rubenstein, P. A. Merz, M. Tonna-DeMasi, R. Fersko, R. I. Carp, H. M. Wisniewski, and H. Diringer. 1987. Mouse polyclonal and monoclonal antibody to scrapie-associated fibril proteins. J. Virol. 61:3688–3693.
31. Manson, J. C., E. Jamieson, H. Baybutt, N. L. Tuzi, R. Barron, I. McConnell, R. Somerville, J. Ironside, R. Will, M.-S. Sy, D. W. Melton, J. Hope, and C. Bostock. 1999. A single amino acid alteration (101L) introduced into murine PrP dramatically alters incubation time of transmissible spongiform encephalopathy. EMBO J. 18:6855–6864.
32. Masters, C. L., D. C. Gajdusek, and C. J. Gibbs, Jr. 1981. Creutzfeldt-Jakob disease virus isolations from the Gerstmann-Sträussler syndrome. Brain 104: 559–588.
33. Moore, R. C., J. Hope, P. A. McBride, I. McConnell, J. Selfridge, D. W. Melton, and J. C. Manson. 1998. Mice with gene targetted prion protein alterations show that *Prnp*, Sinc and *Prni* are congruent. Nat. Genet. 18:118–125.
34. Muramoto, T., S. J. DeArmond, M. Scott, G. C. Telling, F. E. Cohen, and S. B. Prusiner. 1997. Heritable disorder resembling neuronal storage disease in mice expressing prion protein with deletion of an α-helix. Nat. Med. 3:750–755.
35. Peretz, D., R. A. Williamson, Y. Matsunaga, H. Serban, C. Pinilla, R. B. Bastidas, R. Rozenshteyn, T. L. James, R. A. Houghten, F. E. Cohen, S. B. Prusiner, and D. R. Burton. 1997. A conformational transition at the N-terminus of the prion protein features in formation of the scrapie isoform. J. Mol. Biol. 273:614–622.
36. Prusiner, S. B. 1998. Prions. Proc. Natl. Acad. Sci. USA 95:13363–13383.
37. Prusiner, S. B., D. C. Bolton, D. F. Groth, K. A. Bowman, S. P. Cochran, and M. P. McKinley. 1982. Further purification and characterization of scrapie prions. Biochemistry 21:6942–6950.
38. Prusiner, S. B., S. P. Cochran, D. F. Groth, D. E. Downey, K. A. Bowman, and H. M. Martinez. 1982. Measurement of the scrapie agent using an incubation time interval assay. Ann. Neurol. 11:353–358.
39. Safar, J., H. Wille, V. Itri, D. Groth, H. Serban, M. Torchia, F. E. Cohen, and S. B. Prusiner. 1998. Eight prion strains have PrP^{Sc} molecules with different conformations. Nat. Med. 4:1157–1165.
40. Safar, J. G., M. Scott, J. Monaghan, C. Deering, S. Didorenko, J. Vergara, H. Ball, G. Legname, E. Leclerc, L. Solforosi, H. Serban, D. Groth, D. R. Burton, S. B. Prusiner, and R. A. Williamson. 2002. Measuring prions causing bovine spongiform encephalopathy or chronic wasting disease by immunoassays and transgenic mice. Nat. Biotechnol. 20:1147–1150.
41. Scott, M., D. Foster, C. Mirenda, D. Serban, F. Coufal, M. Wälchli, M. Torchia, D. Groth, G. Carlson, S. J. DeArmond, D. Westaway, and S. B. Prusiner. 1989. Transgenic mice expressing hamster prion protein produce species-specific scrapie infectivity and amyloid plaques. Cell 59:847–857.
42. Scott, M. R., R. Will, J. Ironside, H.-O. B. Nguyen, P. Tremblay, S. J. DeArmond, and S. B. Prusiner. 1999. Compelling transgenetic evidence for transmission of bovine spongiform encephalopathy prions to humans. Proc. Natl. Acad. Sci. USA 96:15137–15142.
43. Serban, D., A. Taraboulos, S. J. DeArmond, and S. B. Prusiner. 1990. Rapid detection of Creutzfeldt-Jakob disease and scrapie prion proteins. Neurology 40:110–117.
44. Sparrer, H. E., A. Santoso, F. C. Szoka, Jr., and J. S. Weissman. 2000. Evidence for the prion hypothesis: induction of the yeast [*PSI*$^+$] factor by in vitro-converted Sup35 protein. Science 289:595–599.
45. Taraboulos, A., K. Jendroska, D. Serban, S.-L. Yang, S. J. DeArmond, and S. B. Prusiner. 1992. Regional mapping of prion proteins in brains. Proc. Natl. Acad. Sci. USA 89:7620–7624.
46. Tateishi, J., T. Kitamoto, M. Z. Hoque, and H. Furukawa. 1996. Experimental transmission of Creutzfeldt-Jakob disease and related diseases to rodents. Neurology 46:532–537.
47. Telling, G. C., T. Haga, M. Torchia, P. Tremblay, S. J. DeArmond, and S. B. Prusiner. 1996. Interactions between wild-type and mutant prion proteins modulate neurodegeneration in transgenic mice. Genes Dev. 10:1736–1750.
48. Telling, G. C., M. Scott, J. Mastrianni, R. Gabizon, M. Torchia, F. E. Cohen, S. J. DeArmond, and S. B. Prusiner. 1995. Prion propagation in mice expressing human and chimeric PrP transgenes implicates the interaction of cellular PrP with another protein. Cell 83:79–90.
49. Westaway, D., P. A. Goodman, C. A. Mirenda, M. P. McKinley, G. A. Carlson, and S. B. Prusiner. 1987. Distinct prion proteins in short and long scrapie incubation period mice. Cell 51:651–662.
50. Wille, H., M. D. Michelitsch, V. Guénebaut, S. Supattapone, A. Serban, F. E. Cohen, D. A. Agard, and S. B. Prusiner. 2002. Structural studies of the scrapie prion protein by electron crystallography. Proc. Natl. Acad. Sci. USA 99:3563–3568.